Transferrin Receptor is Required for CD4+ T Cell Iron-Dependent Response During Acute *Toxoplasma gondii* Infection[1]

Stephen L. Denton*, Tathagato Roy*, Martin Akandawen*, Hunter K. Keplinger*, Sai K. Ng*, and Jason P. Gigley*†

*Department of Molecular Biology, University of Wyoming, Laramie, WY, U.S.A.
†Corresponding Author: 307-766-6151, jgigley@uwyo.edu

Abstract

Elemental iron is an essential nutrient involved in many biological processes including infection and immunity. How iron impacts *Toxoplasma gondii* (*T. gondii*) *in vivo* and development of immunity during infection is unclear. We found that although iron is required for parasite proliferation *in vitro,* paradoxically, iron restriction *in vivo* increased parasite burdens during acute and persistent infection stages and decreased survival of mice. Iron restriction lowered IL-12 and IFNγ in spleen and serum, but ratios of myeloid cells and the number and function of Natural Killer cells were unchanged. Iron restriction significantly impaired the development of CD4+ and CD8+ T cell responses to *T. gondii* during replicating type II and attenuated vaccine strain *cps1-1* infection. Low iron conditions reduced the percent and absolute numbers of antigen experienced CD11a+CD49d+, functional IFNγ+, and CD62L-KLRG1+ effector T cells. Iron restriction also decreased vaccine efficacy of *cps1-1* strain against secondary lethal challenge. Antigen experienced CD4+ and CD8+ T cells both upregulated their iron transporter Transferrin receptor 1 (CD71) during infection regardless of iron restriction. Mice whose CD4+ T cells were deficient in CD71 had reduced CD4+ T cell antigen experience and polyfunctionality, yet CD8+ T cell responses remained intact and their long term survival

[1] Funding Sources: NIH 2P20GM103432, R21AI1592, and R21AI1612.

27 was not affected compared to wild type litter mate controls. This study highlights that iron
28 acquisition by T cells is required for activation and vaccine induced long-term protection
29 against *T. gondii*. Understanding how iron affects multiple immune compartments will be
30 essential to define iron regulation of immunity to *T. gondii*.
31
32 List of Abbreviations
33 Transferrin Receptor 1, CD71; Deferiprone, DFP; Toxoplasma Lysate Antigen, TLA;
34 (Days, Weeks) Post Infection, (D,W)PI; T Cell Receptor, TCR; Mean Fluorescent
35 Intensity, MFI; Radical Oxygen Species, ROS; Conditional Knockout of CD71 in CD4+ T
36 Cells; CD4cCD71KO

37 **Introduction**

38 *Toxoplasma gondii (T. gondii)* is an obligate intracellular protozoan parasite
39 infecting about 30% of people world-wide which persists for life and poses a significant
40 health risk (1-3). Understanding the factors that contribute to pathogenesis and
41 development of immunity to this pathogen are critical to develop better vaccines and
42 therapies to treat this infection. *T. gondii* has evolved to rely on scavenging nutrients from
43 the host (4-6). Many of these nutrients are also required for proper development of
44 immune responses to control this infection (7-9). The interplay between parasite
45 nutritional scavenging and immune response development dependent on the same
46 nutrients is poorly understood.

47 Essential metal iron is a nutrient that is utilized both by *T. gondii* and the
48 development of immunity to the parasite. *T. gondii* is highly sensitive to exogenous control
49 of iron levels (10, 11). Treatment of infected cells with IFNγ impairing parasite replication
50 is rescued by iron salt and iron-bearing transferrin (12). A natural function of
51 IFNγ treatment of cells is downregulation of iron uptake receptor Transferrin Receptor
52 (CD71) (13); CD71 in turn is upregulated by *T. gondii* secretions (14). Modulating iron
53 levels in mice infections has been shown to affect intestinal inflammatory damage as well
54 as parasite load (15). However, the long term effects of iron modulation on development
55 of protective immunity to *T. gondii* is not known.

56 Immunity to *T. gondii* is triggered by recognition of the parasite by TLR4 and 11
57 and the production of the proinflammatory cytokine IL-12 (16-20). IL-12 activates group
58 1 Innate Lymphoid Cells including Natural Killer (NK) Cells and ILC1 for the initial
59 production of IFNγ required for early control of *T. gondii* (21-23). After presentation of *T.*

60 *gondii* antigens to T cells by CD8a+ Dendritic cells, both CD4+ and CD8+ T cells mount
61 a robust response producing high levels of IFNγ (24). CD8+ T cells, *via* their
62 IFNγ production, emerge to become the dominant cell required for long-term protection
63 against the infection. CD4+ T cells are required continuously to help maintain CD8+ T
64 cell dependent protection (25, 26). Despite induction of a robust CD8+ T cell response,
65 immunity to *T. gondii* is not sterilizing and the parasite escapes to develop a persistent
66 infection in skeletal muscle and the central nervous system (27). Part of the inability of
67 CD8+ T cells to clear the persistent infection is the development of immune exhaustion
68 (27-29). The immune exhaustion of CD8+ T cells maybe partially dependent upon CD4+
69 T cells responding to the infection, highlighting that CD4+ T cells can be essential but
70 also detrimental to long term CD8+ T cell dependent protection (26, 30). The
71 immunological reasons why the parasite is not completely cleared is still not well defined.
72 Available iron could be an important factor required in this process.

73 Iron-dependent roles in immunity include neutrophil extracellular trap formation
74 (31), macrophage polarization (32, 33), dendritic cell maturation (34), and NK cell target
75 recognition (35, 36). T Cell proliferation and IL-2R upregulation during activation is also
76 dependent on intracellular iron levels (37) and CD71-dependent iron uptake (38). T-helper
77 type 1 (Th1) but not Th2 cytokine production is also dependent on iron status (39, 40),
78 indicating that relative iron levels could be a sensing mechanism for T-helper type
79 differentiation. Much of what is known about iron and immunity is in the absence of
80 infection. How iron regulates infection pathogenesis and development of immunity during
81 infection including *T. gondii* infection *in vivo* is unclear.

82 We investigated how limiting iron during infection in a murine model impacted
83 infection pathogenesis and immunity to *T. gondii*. Similar to previously published studies,
84 we observed that limiting iron *in vitro* slowed the proliferation of the parasite. However,
85 unlike other studies we observed that there was increased morbidity and mortality of the
86 animals in iron limiting conditions, and the parasite disseminated better to the CNS to
87 develop a much higher persistent cyst burden than normal iron conditions. To examine
88 the role of iron in *T. gondii* resistance, we observed that splenic and serum production of
89 IL-12p40 and IFNγ by 5 days after infection were inhibited by iron restriction, but the
90 proportions of spleen leukocytes and NK production of IFNγ were unaffected. However,
91 the expansion of antigen experienced CD4+ and CD8+ T cells responding to infection
92 was dependent on iron availability. Consequently, the Th1 polyfunction (TNFα and IFNγ
93 production) of the CD4+ T cells was inhibited by iron restriction in *T. gondii* infection.
94 Inhibition of T cell responses by iron restriction was independent from antigen load and
95 impacted development of long-term vaccine induced protection. CD4+ T cell specific
96 expression of CD71 was intrinsically required for antigen experience and polyfunction of
97 CD4+ and not CD8+ T cells, yet conditional CD71 knockout mice were not more
98 susceptible to *T. gondii* infection. These results demonstrate the importance of iron in
99 global development of protective immunity to *T. gondii* but also that iron-sensing by CD71
100 regulates CD4+ T cell activation is a critical component of long-term immunity to *T. gondii*
101 infection.
102

Materials and Methods

Ethics Statement

All animal husbandry and experiments were performed by the Gigley Laboratory at the University of Wyoming in strict accordance to the guidelines approved by the University of Wyoming Institutional Animal Care and Use Committee.

Mouse strains, parasite propagation, and infections

C57BL/6J (#000664), RAG1-/- (B6.129S7-Rag1$^{tm1Mom/J}$, #002216), and CD4-CreER^{T2} (B6(129X1)-Tg(Cd4-cre/ERT2)11Gnri/J, #022356) mice were purchased from Jackson Laboratories. CD71$^{Flx/Flx}$ mice were a kind gift from Mark Andrews, Harvard University. CD4-CreER^{T2} mice were crossed with CD71$^{Flx/Flx}$ for two generations and the resulting progeny were interbred to produce CD4-CreER^{T2} +/-::CD71$^{Flx/Flx}$. The genomes of these mice contained 75% C57BL/6 heritage from the CD4-CreER^{T2} parentage and 25% 129 heritage from the CD71$^{Flx/Flx}$ parentage, thus, all experiments using these mice used internal littermate controls. Mouse genotypes were assessed by PCR from genomic DNA isolated from ear clips *via* digestion in DirectPCR Digestion Buffer + Proteinase K (Viagen Biotech) using the following primer pairs: CD4-CreER^{T2} Forward (0.5μM): 5'-GCG GTC TGG CAG TAA AAA CTA TC -3', CD4-CreER^{T2} Reverse (0.5μM): 5'- GTG AAA CAG CAT TGC TGT CAC TT -3', and separately TfR^{Flx} Forward (0.3μM): (5'-TTC AGT TCC CAG TGA CCA CA -3'), TfR^{Flx} Reverse (0.3μM): 5'- TCC TTT CTG TGC CCA GTT CT -3'. The CD4-CreER^{T2} transgene was detected by a 100nt PCR product. The 310nt lox-containing CD71 allele was differentiated from the 165nt wild-type CD71 allele by gel electrophoresis. Female mice aged 8-12 weeks old were used for all experiments.

125 Type II *T. gondii* ME49 strain was maintained by serial passage in CBA mice
126 (Jackson Laboratories #000656). Cyst numbers were counted in 10μL of brain
127 homogenate from previously infected animals placed on a glass microscope slide. Mice
128 were inoculated intragastrically (i.g.) with 7-10 cysts in 200μL Phosphate-Buffered Saline
129 (PBS) via oral gavage.

130 Type I *T. gondii* RH strain was maintained by routine passage in MRC5 fibroblasts
131 in 1 % Dulbecco's Modified Eagles Medium (1% DMEM) (1% Fetal Bovine Serum, 1X
132 Penicillin/Streptomycin, 1X Amphotericin B). Upon lysis of MRC5 monolayers,
133 tachyzoites were purified by 3μm filtration and enumerated on a hemocytometer. 1 X 10^3
134 parasites were injected intraperitoneally (i.p.) in 200μL PBS. Attenuated Type I *T. gondii*
135 strain *cps1-1* (CPS) was maintained by routine passage in MRC5 fibroblasts in 1% DMEM
136 supplemented with 300mM uracil. Following filtration and enumeration similar to RH
137 cultures, CPS was injected i.p. with a 27G needle at parasite concentrations as indicated
138 in 1 X PBS.

139 *Drug Formulation and Treatment*

140 Deferiprone (3-Hydroxy-1,2-dimethyl-4(1H)-pyridone "DFP", Sigma-Aldrich
141 #379409, CAS #30652-11-0) was dissolved at 10mg/mL in distilled water at 37˚C and
142 sterilized by filtration through a 0.2μm membrane. Each preparation was tested for Iron-
143 Binding Units using a colorimetric Iron Assay Kit (Abcam Cat #ab83366) according to the
144 manufacturer's instructions. Briefly, a standard curve was created using a known amount
145 of iron was prepared in Assay Buffer, and variable volumes of DFP preparations were
146 added to replicates of the top standard. Iron reducer was added to every sample to
147 measure total free iron in the solution. After addition of the iron probe, the absorbance of

148 the samples was measured at 593nm and the amount of free iron remaining in the sample
149 was extrapolated from the standard curve. The volume of DFP from each preparation
150 required to reduce the iron in the samples by 50% was deemed an Iron-Binding Unit (U).
151 DFP was administered at 75U per mouse intraperitoneally with a 27G needle every other
152 day starting the day preceding infection, unless otherwise indicated.

153 Tamoxifen (Sigma-Aldrich #T5648, CAS #10540-29-1) was dissolved at 20mg/mL
154 in corn oil (Sigma-Aldrich #C8267, CAS #8001-30-7) overnight by agitation at 37˚C in the
155 dark. Tamoxifen was administered at 100mg/kg to mice intraperitoneally with a 27G
156 needle daily for the five days preceding infection.

157 *ELISA*

158 Blood samples were collected by retroorbital bleeding of isoflurane anesthetized
159 mice, followed by a coagulation period for 30 minutes at room temperature. Serum was
160 collected after centrifugation. Splenic samples were suspended at $5*10^6$ cells per well in
161 FACS Media and incubated for 48 hours at 37˚C and 5% CO_2. Cells were lysed by 3X
162 freeze/thaw cycles at -80˚C, and supernatant isolated for ELISA. Both serum and spleen
163 samples were diluted at a volume of 1:20 for IL-12p40 and 1:15 for IFNγ ELISAs, which
164 were performed according to manufacturer instructions using kits for IL-12p40 (Biolegend
165 431604) and IFNγ (Biolegend 430804).

166 *Parasite Burdens by Genome Equivalence*

167 Genomic DNA from specified organs was purified from the samples using the DNeasy
168 Blood & Tissue Kit (Qiagen 69506) according to manufacturer instructions. A standard
169 curve of known quantity of RH gDNA was assessed alongside 100ng-400ng of sample
170 DNA as template to query for the *T. gondii* unique gene B1 using SSO Advanced SYBR

171 Master Mix (Bio-Rad 1725017) and 0.5μM primers (F: 5'- CGT CCG TCG TAA TAT CAG
172 -3', R: 5'- GAC TTC ATG GGA CGA TAT G -3'). The thermocycler conditions were 1:
173 95˚C for 10 minutes, 2: 95˚C for 5 seconds, 3: 60˚C for 5 seconds, 4: 72˚C for 5 seconds
174 + plate read, 5: Cycle 2-4, 44 repetitions, 6: Melt Curve 65˚C to 95˚C with 0.5˚C, 5 second
175 increments + plate read. Parasite concentrations were extrapolated from linear regression
176 of the standard curve.

177 *Plaque Assay*

178 MRC5 fibroblasts were seeded into 6-well tissue culture plates and treated with
179 DFP or ferric citrate as indicated immediately prior to infection. 100 RH parasites were
180 inoculated per well and incubated for 7 days at 37˚C and 5% CO_2. Monolayers were fixed
181 with 100% EtOH and stained with Plaque Assay Stain (125mL of 10% Crystal Violet in
182 EtOH w/v + 500mL 1% Ammonium Oxalate w/v). Plaques were visualized by projection
183 using a Bellco Glass, Inc. Slide Magnifier and manually counted. Plaque size was
184 estimated as a measurement of $A = \pi * m((LA+TA)/4)^2$, where A = Area (mm2), m =
185 magnification factor, LA = length of longest axis of plaque (mm), and TA = length of
186 transverse axis perpendicular to the longest axis (mm). Representative images were
187 taken with an Apple® iPhone Xr and background digitally removed with Adobe®
188 Photoshop.

189 *Single Cell Suspension*

190 For peritoneal exudate cells (PEC), the peritoneum of mice was exposed intact,
191 and injected with 10mL Stain/Wash Buffer with EDTA (SWBE, 5% w/v Bovine Calf Serum
192 and 2mM EDTA in PBS) *via* a 21G needle. Cells were dislodged by external agitation of
193 the cavity during gradual injection of the SWBE and redrawn in the syringe. Spleens were

194 extracted and crushed through a 70μm cell strainer with SWBE washing, followed by
195 osmotic lysis of red blood cells (RBC) by suspension in 1mL 1X RBC Lysis Buffer (Tonbo
196 Biosciences #TNB-4300-L100) for 3 minutes. RBC lysis was quenched by addition of
197 20mL SWBE, and samples were passed through a 70μm cell strainer. Single cell
198 suspension concentrations were estimated with a hemocytometer.

199 *Flow Cytometry- Minimal Information About T Cell / Natural Killer Cell Assays (MIATA-*
200 *MIANKA)*

201 Single cell suspensions were aliquoted to a clear FACS V-bottom plate at one
202 million cells per well. Cell viability was estimated using LIVE/DEAD Fixable Aqua dye
203 (ThermoFisher L34957), followed by extracellular antibody staining in SWBE, fixation and
204 permeabilization by BD Cytofix/Cytoperm (BD Biosciences 554714), and intracellular /
205 secondary staining in BD Perm/Wash buffer, all according to manufacturer instructions.
206 Samples were processed in Guava EasyCyte 12HT Flow Cytometer and analyzed in
207 FlowJo v.9.7.7 software.

208 For NK Cell assays, wells were coated with 0.5μg per well of NK1.1 (PK136,
209 BioXCell BE0036) overnight at 4˚C the day prior to staining. After plating in coated wells,
210 cells were stimulated at 37˚C and 5% CO_2 four 4 hours with 0.66X Protein Transport
211 Inhibitor Cocktail (PTIC, eBioscience 00-4980-03) in FACS Media (Isocove's DMEM with
212 L-Glutamine and 25mM HEPES supplemented with 1X Penicillin/ Streptomycin,
213 Amphotericin B, Non-Essential Amino Acids, 0.1mM Sodium Pyruvate, 0.2mM Glutamine
214 XL, 10% Fetal Bovine Serum, and 0.1mM 2-mercaptoethanol). Extracellular stain
215 included CD3-FITC (17A2, Biolegend 100204), CD335/NKp46-APC (29A1.4, Biolegend
216 137608), and CD49b-Biotin (DX5, Biolegend 108904). Intracellular / secondary stain

217 included IFNγ-PE (XMG1.2, Biolegend 505806) and Streptavidin-PE/Cy7 (Biolegend
218 405206). cNK cells were boolean gated on live cells by Live/Dead Aqua, lymphocytes by
219 scatter profile, and as CD3-, CD49b+, and NKp46+.

220 For T Cell phenotype assays, cells were plated and proceeded with direct *ex vivo*
221 staining. Extracellular stain included CD4-BV421 (GK1.5, Biolegend 100438), CD8-
222 PE/Cy5 (53-6.7, Biolegend 100710), CD11a-PE/Cy7 (I21/7, Biolegend 153108), CD62L-
223 APC/Cy7 (MEL-14, Biolegend 104428), CD49d-PE (9C10/MFR4.B, Biolegend 103706),
224 KLRG1-PE (2F1/KLRG1, Biolegend 138408), KLRG1-APC (2F1/KLRG1, Biolegend
225 138412), CD71/TfR1-APC (RI7217, Biolegend 113820), and intracellular stain Ki67-PE
226 (16A8, Biolegend 652404). Cells were boolean gated on live cell by Live/Dead Aqua,
227 lymphocytes by scatter profiling, and either CD4+/CD8- or CD4-/CD8+.

228 For T cell function assays, cells were plated in FACS media supplemented with
229 4µg Toxoplasma Lysate Antigen (TLA) per test and stimulated for 8 hours at 37˚C and
230 5% CO_2. For the last 4 hours of stimulation, PTIC was added to each well at a final
231 concentration of 1X. Extracellular staining included CD4-BV421 (GK1.5, Biolegend
232 100438) and CD8-PE/Cy5 (53-6.7, Biolegend 100710), and intracellular staining included
233 IFNγ-PE (XMG1.2, Biolegend 505806), TNFα-APC (MP6-XT22, Invitrogen 17-7321-82),
234 and GZB-FITC (QA16A02, Biolegend 372296). TLA was produced by sonication of
235 purified RH strain *T. gondii* parasites in PBS, and the concentration was determined by
236 Bradford Assay. Cells were boolean gated on live cell by Live/Dead Aqua, lymphocytes
237 by scatter profiling, and either CD4+/CD8- or CD4-/CD8+.

238 For fluorescence activated cell sorting, 20 million cells per tube were assessed for
239 cell viability by Live/Dead Aqua and stained without fixation with CD3-PE (17A2,

240 Biolegend 100206) and CD4-FITC (GK1.5, Biolegend 100406). Samples were processed
241 in a BD FACSMelody Cell Sorter before immediate RNA isolation. Sorting strategy is
242 defined in Figure S4.

243 For splenic profiling screens, extracellular stain proceeded immediately *ex vivo*
244 and the following antibodies were used: CD3-BV421 (17A2, Biolegend 100228), CD19-
245 BV605 (6D5, Biolegend 115540), NK1.1-FITC (PK136, Biolegend 108706), CD11b-APC
246 (M1/70 Biolegend 101212), Ly6C-PE (HK1.4, Biolegend 128008), Ly6G-PE/Cy7 (1A8,
247 Biolegend 127618), CD11c-FITC (N418, Biolegend 117306), and I-E/I-A-PE
248 (M5/114.15.2, Biolegend 107608). Gating strategy is defined in Figure 3A.

249 *RNA Isolation and qRT-PCR*

250 Samples collected in FACS experiments were pelleted and resuspended in TRI Reagent
251 (Sigma T9424) for RNA Isolation according to manufacturer instructions. RNA was further
252 purified by RNA Cleanup Protocol of RNeasy Kit (Qiagen 74104). RNA samples were
253 quantified by UV absorbance and cDNA synthesis was performed on normalized mass
254 (50ng P1 samples, 20ng P2 samples) of RNA according to manufacturer instructions with
255 Superscript IV Reverse Transcriptase (Invitrogen 18091050). Equal volumes of cDNA
256 samples were used in qRT-PCR reactions using Sso Advanced Universal SYBR Master
257 Mix (Bio-Rad 1725271) and validated primers (41, 42): Actin Forward (0.5μM) 5'- ACC
258 CAC ACT GTG CCC ATC TA -3', Actin Reverse (0.5μM) 5'- CAC GCT CGG TCA GGA
259 TCT TC -3', CD71 Forward (0.5μM) 5'- TCA AGC CAG ATC AGC AAT TCT C -3', and
260 CD71 Reverse (0.5μM) 5'- AGC CAG TTT CAT CTC CAC ATG - 3'. The PCR protocol
261 was 1: 95˚C for 3:00, 2: 95˚C for 0:15, 60˚C for 0:15, 72˚C for 1:20 + Plate Read, 5:

262 Repeat 2-5 44X, 6: Melt Curve 65.0˚C to 95.0˚C, 0.5˚C increment for 0:05 + Plate Read.
263 mRNA ratios were estimated using the ΔΔCt method.

264 *Statistical Analysis*

265 Statistics and graph generation were completed using Graphpad Prism v.9 and
266 Microsoft Excel v16.54 software. Experiments are pooled from at least two independent
267 technical repeats containing 3-5 replicates per experiment. Statistics were performed
268 between two groups by Student's t-test or between multiple groups by One-Way ANOVA,
269 or by Kaplan-Meier Survival analysis. Significance is indicated by *$p<0.05$, **$p<0.01$,
270 ***$p<0.005$, and ****$p<0.001$. Figures were assembled in Adobe Illustrator 2021,
271 references in Endnote X8.

272

273 Results

274 ***Iron is an essential nutrient for Toxoplasma gondii***

275 To study the roles of iron in *Toxoplasma gondii* pathogenesis and immunity, it was
276 necessary to induce a rapid depletion of iron at the onset of an infection. To this end, we
277 selected use of the small molecule cell permeable iron chelator deferiprone (DFP) (43).
278 Based on lot-to-lot differences of iron chelation ability, we developed experimental
279 reproducibility by normalization of iron-binding efficiency in each formulation. In this
280 assay, the redox ability of free iron reacts with Ferense S, a chromogen to produce a
281 colorimetric readout linearly correlated with free iron concentration. We challenged a
282 known amount of iron, 10nM, with a range of DFP amounts by batch. The required mass
283 of each formulation to decrease the free iron to 5nM, or 50% binding, was deemed an
284 Iron-Binding Unit (U) (Figure 1A).

285 Dose titrating DFP into an infection setting showed a dose-dependent inhibition of
286 parasite replication by plaque assay (Figure S1A) both in plaque number (Figure S1B)
287 and plaque size (Figure S1C). The minimal dose tested that was sufficient to completely
288 prevent plaque formation was 1.37U DFP, therefore, we tested this amount of DFP in a
289 titration of a range of ferric citrate supplementation. A minimal dose of 20μg ferric citrate
290 was sufficient to rescue the inhibition of parasite growth (Figure S1D). Lower doses of
291 ferric citrate alone did not increase numbers of plaques observed (Figure S1E). However,
292 at higher doses, which overcame DFP inhibitory effects, ferric citrate alone displayed
293 toxicity to the host monolayer integrity (Figure S1A). This agrees with previous studies
294 demonstrating the role of vacuolar Iron transporter (VIT) being important for regulating

295 iron homeostasis in *T. gondii* (10). In summary experiments, DFP prevented *T. gondii*
296 plaque formation in an iron-dependent manner (Figure 1B-C).

297 ***Iron restriction "therapy" increases morbidity and mortality of T. gondii infection***

298 Given the parasite-inhibitory properties of DFP *in vitro* we tested how iron chelation
299 with DFP impacted infection pathogenesis *in vivo*. DFP is currently used in human
300 patients as a safe iron overload therapy (43). During Type II ME49 strain infection in
301 mice, treatment with DFP resulted in increased weight loss and mortality compared to
302 non-treated controls (Figure 1D-E). The difference between iron chelation inhibition of
303 proliferation *in vitro* and increased morbidity and mortality *in vivo* was surprising.
304 Therefore we measured acute parasite burden in tissues of infected mice acute (14 DPI)
305 and chronic (5 weeks PI, 5WPI) infection (20). DFP unexpectedly increased
306 dissemination by 4-fold as assessed by parasite burden in the lung at 14DPI (Figure 1F),
307 and by encystation in the brain at 5WPI (Figure 1G). These results indicate DFP restriction
308 of iron impacts not only parasite proliferation, but dissemination and possibly
309 development of immunity to *T. gondii*.

310 ***IL-12 and IFNγ production is reliant on available iron in acute infection***

311 IL-12 dependent IFNγ production is the key pathway for resistance to *T. gondii*, but
312 also may contribute to inflammatory tissue damage (18, 22, 44). Therefore, changes in
313 expression of these cytokines could correlate with the increased pathogenesis due to
314 DFP-induced iron restriction. To determine how DFP treatment impacted development of
315 immune control to *T. gondii* we compared IL-12 and IFNγ levels in naïve mice, ME49
316 infected mice and mice infected with ME49 and treated with DFP. As expected, *T. gondii*
317 infection significantly increased IL-12 and IFNγ in spleen cells (IL-12: 17-fold, IFNγ: 32-

318 fold) and serum (IL-12: 4-fold, IFNγ: 9-fold) compared to naïve animals (Figure 2). Iron
319 restriction by DFP treatment significantly lowered the levels of these cytokines in both
320 spleen cells and serum. These observations suggest that iron is a key factor in the
321 activation of the immune response to *T. gondii*.

322 ***Iron restriction does not impact splenocyte composition in acute infection***

323 Because we observed significantly lower IL-12 and IFNγ during the early acute
324 infection we further explored innate immune cell recruitment at this stage of infection.
325 Neutrophils, Monocytes, Macrophages and Dendritic cells are all important producers of
326 IL-12 (45, 46). Group 1 ILCs including natural killer cells and ILC1 are important early
327 sources of IFNγ to initiate control of *T. gondii* (21-23). Analysis of spleen immune cell
328 composition during acute ME49 infection with and without iron restriction by DFP revealed
329 that restricting iron availability with DFP treatment (Figure 3A-B) did not have a significant
330 impact on the frequencies of (CD19+ CD3-) B cells (Figure S2B), (CD19- CD3+ NK1.1-)
331 T Cells (Figure S2C), (CD19- CD3- NK1.1+) NK Cells (Figure S2D), (Lineage- CD11b+
332 Ly6Chi Ly6G-) inflammatory monocytes (Figure S2E), (Lineage- CD11b+ Ly6Cint Ly6G+)
333 neutrophils (Figure S2F), and (Lineage- CD11c+ MHCII+) Dendritic cells (Figure S2G).
334 Notably, the total live lymphocyte numbers in spleen were significantly reduced at 5DPI
335 only in iron restricted and infected animals, from $5.5\text{-}6*10^7$ cells to $4*10^7$ (Figure S2A).
336 These results suggested that the overall composition of splenocytes could not explain the
337 differences in morbidity, mortality and dissemination.

338 To further test if the innate cell composition is affected by iron restriction, we
339 infected $Rag1^{tm1Mom}$ (RAG1-/-), mice which are deficient in adaptive B or T cells (47), with
340 cysts of ME49. RAG1-/- mice started to succumb to the infection starting at 2-3 WPI,

341 however, iron restriction by DFP treatment during infection of these animals did not
342 significantly change the mortality of the infection (Figure 3C). Taken together, these
343 results suggest that the level of available iron impacts some innate immune cell function,
344 but not cellular composition during acute *T. gondii* infection.

345 ***Iron does not regulate NK cell number or IFNγ production.***

346 NK cells are critical for early T cell independent control of *T. gondii* infection (18,
347 21, 22, 48, 49). Even though there was no difference in mortality due to iron restriction in
348 RAG1-/- animals who have an intact NK cell compartment, there was a significantly
349 impaired systemic IFNγ production in WT animals. Therefore, we assayed NK cell (CD3-
350 CD49b+ NKp46+) function in the presence or absence of iron restriction with DFP at 5
351 DPI in the spleen. The frequency and number of the NK cells dropped significantly during
352 acute infection compared to naïve animals. However, the decrease in NK cells was
353 similar regardless of DFP treatment (Figure 4A). NK cells were activated to produce IFNγ
354 regardless of iron restriction by DFP suggesting that NK cells do not rely on available iron
355 levels for their response (Figure 4B).

356 ***Iron is required to generate antigen experienced CD4+ and CD8+ T cells***

357 Our results above suggest innate immune cell activity during iron restriction with
358 DFP is relatively intact leading us to hypothesize that iron regulates and is essential for
359 development of adaptive immune responses to *T. gondii*. We tested this hypothesis by
360 examining the CD4+ and CD8+ T cell responses at the beginning of the adaptive
361 response at 10 DPI with ME49 cysts by flow cytometry (50, 51). As expected, the
362 frequency and number of total splenic helper CD4+ and cytotoxic CD8+ T cells was
363 reduced after *T. gondii* infection compared to naïve animals (Figure 5A). In the iron-

364 restricted infection group, this reduction in CD4+ and CD8+ T cells was comparable
365 (Figure 5A). To better determine whether and how iron regulates T cell responses to *T.*
366 *gondii* infection, antigen experienced T cells were assayed by flow cytometry. T cell
367 upregulation of CD11a and tandem expression of CD49d is strongly correlated with
368 markers of activation, thus, CD11a and CD49d (CD11a(Hi) CD49d+) serve as efficient
369 surrogate markers of antigen experience (52). The frequency of the CD11a(Hi) CD49d+
370 population of antigen experienced CD4+ T cells increases from 5.7% in naïve animals to
371 47.3% in *T. gondii* infected animals without iron restriction (Figure 5B). Similarly, the
372 frequency of CD11a(Hi) CD49d+ CD8+ antigen experienced T cells increased from 5.6%
373 to 43.8% after *T. gondii* infection without iron restriction (Figure 5C). Absolute numbers
374 of antigen experienced CD4+ and CD8+ T cells also increased significantly after infection
375 in non-DFP treated animals compared to naïve controls (Figure 5B-C). However, the
376 frequency of antigen experienced cells only reached 27.4% in CD4+ T cells and 22.1%
377 in CD8+ T cells (Figure 5B-C). Moreover, the absolute number of antigen experienced
378 CD4+ and CD8+ T cells under iron restriction was not significantly higher than in the naïve
379 group. Iron restriction by treating animals with DFP during infection thus significantly
380 inhibited increases in both the frequency and absolute number of antigen experienced
381 CD11a(Hi) CD49d+ T cells compared to naïve and infected non-DFP treated animals.

382 ***Iron is required for functional CD4+ T cell polyfunctional response***

383 Due to the inhibitory effect of iron restriction on increases in T cell antigen
384 experience, it was likely that the functions of these cells were also inhibited. Therefore
385 we measured function of CD4+ (IFNγ and TNFα) and CD8+ T cells (IFNγ) *ex vivo* from
386 mice infected with ME49 and treated or not with DFP to restrict iron (53-57). The

387 frequency of polyfunctional IFNγ+ / TNFα+ CD4+ T cells increased from 0.017% to 13.8%
388 after infection (Figure 5D). Additionally, the frequency of IFNγ-producing CD8+ T cells
389 increased from 0.44% in naïve to 8.7% after infection (Figure 5E). The inhibitory effect of
390 iron restriction on antigen experience in CD4+ T cells translated to inhibited function, as
391 the frequency of polyfunctional CD4+ T cells was 6.5%, significantly lower than untreated
392 infected animals, but still significantly higher than naïve animals (Figure 5D). In contrast,
393 iron restricted animals still mounted a functional CD8+ T cell response, as the frequency
394 of IFNγ+ CD8+ T cells (6.1%) was not significantly different than in untreated infection
395 (Figure 5E).

396 ***Antigen experienced CD4+ and CD8+ T cells upregulate CD71 expression***

397 CD71 mediates iron uptake in most mammalian cell types, including immune cells
398 (58). Additionally, CD71 is both upregulated and required for T cell activation *in vitro* (59-
399 61). To link the inhibitory effect of iron restriction on T cell responses to T cell intrinsic iron
400 uptake, we measured CD71 expression levels on CD4+ and CD8+ T cells during *T. gondii*
401 infection using flow cytometry (Figure 5F-I). We observed a significant 2.7-fold increase
402 in CD71 MFI on CD4+ T cells and a 2.4-fold increase on CD8+ T cells during *T. gondii*
403 infection. In iron restricted animals, CD71 MFI of total CD4+ or CD8+ T cells was not
404 significantly different compared to untreated infection groups (Figure 5F-G). We next
405 measured CD71 MFI in antigen experienced CD11dHi CD49a+ T cells. Similar to total
406 CD4+ and CD8+ T cells, CD71 increased in expression after *T. gondii* infection on
407 CD11dHi CD49a+ antigen experienced CD4+ and CD8+ T cells compared to naïve
408 conditions (Figure 5H-I). The MFI of CD71 was significantly higher on antigen
409 experienced CD4+ and CD8+ T cells on a per cell basis (Figure 5H-I) than total CD4+

410 and CD8+ T cells (Figure 5F-G) from both non-DFP treated and iron restricted DFP
411 treated infected mice. Iron restriction by DFP treatment also significantly increased CD71
412 MFI on antigen experienced CD4+ T cells compared to cells from non-treated infected
413 animals (Figure 5H). Interestingly, iron restriction by DFP treatment did not impact the
414 CD71 MFI of antigen experienced CD8+ T cells (Figure 5I). These results show that CD71
415 is upregulated on T cells during *T. gondii* infection, and that iron restriction by DFP
416 treatment further upregulates CD71 only in antigen experienced CD4+ T cells.

417 ***Iron restriction reduces frequency of effector CD8+ T cell subsets***

418 Iron restriction significantly decreased the number of antigen experienced CD8+ T
419 cells during *T. gondii* infection. To provide control of the parasite, CD8+ T cells
420 differentiate from naïve (CD62L+KLRG1-, FI) into memory precursor (CD62L-KLRG1-,
421 FII), short lived effector cell (CD62L-KLRG1Hi, FIII), and CD62L+ effector cells
422 (CD62L+KLRG1+, FIV) (Figure 5J) (62). Therefore we measured CD8+ T cell
423 differentiation in the presence or absence of iron restriction by DFP treatment during *T.*
424 *gondii* infection defined by functional output (Figure 5J). The frequency of the naïve FI
425 population decreased after infection from 93.55% of naïve animals to 62.65% in normal
426 iron condition (non-DFP treated) animals. In the iron restricted (DFP-treated) group, there
427 was a significantly greater proportion of CD8+ T cells remaining naïve at 75.73%
428 compared to non-treated infected mice. After infection in non-DFP treated mice, CD8+ T
429 cells differentiated into FII memory precursor subset (CD62L- KLRG1-, 13.38%), the FIII
430 effector subset (CD62L- KLRG1+, 13.06%), and the FIV CD62L+ effector subset
431 (CD62L+ KLRG1+, 10.89%). Iron restriction by DFP treatment inhibited differentiation of
432 FIII (6.01%) and FIV (5.61%) effector subsets, both of which were significantly lower than

433 in untreated infection and higher than naïve mice. However, the proportion CD8+ T cells
434 belonging to the FII memory precursor subset (12.65%) was not significantly different
435 between the DFP-treated or non-treated infection groups.

436 ***Reduced T cell activation during iron restriction is independent of antigen load and***
437 ***occurs during vaccination.***

438 One of the reasons we may observe decreased antigen experienced CD4+ and
439 CD8+ T cells and CD4+ T cell polyfunctional responses is the lack of sufficient *T. gondii*
440 antigen due to the possibility that iron restriction slows *T. gondii* growth *in vivo*. The
441 quantity and quality of antigen load is linked to differences in T cell activation and
442 protection in *T. gondii* infection (25, 63, 64). Therefore to control for differences in antigen
443 levels that might cause defects in T cell responses during DFP induced iron restriction,
444 we immunized mice i.p. using 1 X 10^6 tachyzoites of the non-replicating vaccine strain of
445 *T. gondii,* CPS (24, 65) with or without DFP induced iron restriction. We analyzed the
446 CD4+ and CD8+ T cell responses at the site of infection (PEC, Figure 6) and the systemic
447 response on day 7 p.i. (spleen, Supplemental Figure 3).

448 In the PEC, the frequency and absolute number of total CD4+ and CD8+ T cells
449 increased after vaccination (Figure 6A). Iron restriction using DFP significantly reduced
450 those increases and were not significantly greater than naïve mice (Figure 6A). The
451 frequency and number of antigen experienced (CD11aHi CD49d+) CD4+ and CD8+ T
452 cells were then measured in the PEC of vaccinated mice with and without DFP iron
453 restriction. In naïve animals, there was a high baseline frequency of CD11a(Hi) / CD49d+
454 antigen experienced CD4+ and CD8+ cells. The frequency and absolute number of
455 antigen experienced CD4+ and CD8+ T cells significantly increased in response to

456 vaccination with CPS compared to naïve controls (CD4+ frequency: 2.33-fold, number:
457 7.31-fold and CD8+ frequency: 2.13-fold, number: 7.43-fold). In contrast, DFP induced
458 iron restriction resulted in a near complete inhibition of increased antigen experienced
459 CD4+ T cell populations with only 1.13-fold (frequency) and 1.38-fold (number) non-
460 significant increases after vaccination (Figure 6B). Similarly, DFP induced iron restriction
461 inhibited CD8+ T cell populations with 1.67-fold (frequency) and 2.15-fold (number) non-
462 significant changes compared to unvaccinated groups (Figure 6C). Consequently, we
463 measured CD4+ T cell polyfunction (IFNγ+/TNFα+) and CD8+ T cell single function
464 (IFNγ+) after CPS vaccination. Both the frequency and absolute number of single and
465 polyfunctional CD4+ and CD8+ T cells were significantly increased after vaccination in
466 the PEC. DFP induced iron restriction significantly reduced CD4+ and CD8+ T cell
467 functions in both frequency and absolute number, and for CD8+ T cells, frequency and
468 absolute number of functional cells were not significantly different from naïve animals
469 (Figure 6D-E).

470 We next measured the ratio of naïve (CD62L+KLRG1-, FI), memory precursor
471 (CD62L-KLRG1-, FII), short lived effector (CD62L-KLRG1+, FIII), and CD62L+effector
472 (CD62L+KLRG1+, FIV) CD8+ T cells in PEC of naïve, CPS immunized/non-treated and
473 CPS immunized/DFP-treated iron restricted mice (Figure 6F). We observed an increase
474 in naïve CD8+ T cells (FI) after CPS vaccination compared to non-immunized animals
475 and iron restriction further increased the frequency of these cells compared to naïve and
476 CPS alone. Memory precursor CD8+ T cells (FII) decreased significantly after CPS
477 vaccination with or without DFP treatment and DFP did not affect this decrease. The
478 frequency of effector CD8+ T cells (FIII) increased significantly after CPS vaccination

479 compared to naïve animals and DFP induced iron restriction significantly decreased this
480 cell population to lower levels than naïve and CPS infected mice. There was only a
481 moderate effect on CD8+ CD62L+ effector T cells with CPS immunization and CPS with
482 DFP treatment compared to naïve mice.

483 In the spleen, the response to CPS is more subtle due to the localized immune
484 response induced by this parasite strain in the PEC (62, 66). Measuring the CD4+ and
485 CD8+ T cell responses in the periphery revealed that even though the frequency and
486 absolute number of total T cells were unchanged (Figure S3A), antigen experience and
487 function increased significantly after vaccination (Figure S3B-E). Similar to PEC these
488 increases were inhibited in DFP induced iron restriction conditions and were not greater
489 than naïve mouse cells. These results demonstrate that iron-restriction in CPS
490 vaccination when antigen availability is normalized still significantly decreases T cell
491 responses similar to ME49 infection, revealing the role of iron as a critical factor involved
492 for the proper activation of T cell immunity to *T. gondii* independent of antigen level.

493 ***Iron-restricted inhibition of adaptive immunity also reduces vaccine induced long-***
494 ***term protective immunity against lethal T. gondii rechallenge.***

495 Iron-restriction inhibits CD4+ and CD8+ T cells responses during primary infection
496 of both ME49 and CPS strains. How iron impacts development of long term memory and
497 control of *T. gondii after* vaccination with CPS has not been tested. CPS vaccination
498 induces robust T cell memory that is highly protective against lethal challenge (25). Mice
499 were immunized with a dose titration of CPS (5×10^4, 1×10^5, and 5×10^5) tachyzoites
500 and treated or not with DFP for the first three weeks after vaccination. Mice were then
501 allowed to recover without DFP treatment to re-establish normal iron homeostasis for two

502 weeks. All mice were then challenged with a lethal dose (1 X 10^3) of the Type I CPS
503 parental strain RH i.p and monitored for survival. As shown in Figure 6E, 5 X 10^4
504 tachyzoites were not protective and 1 X 10^5 were partially protective against lethal
505 challenge. 5 X 10^5 CPS tachyzoites induced near-complete protective immunity to lethal
506 challenge. DFP induced iron restriction decreased CPS vaccine dose efficacy in both 1
507 X 10^4 and 5 X 10^5 CPS animals. This result demonstrates that iron is critical during
508 immunization and iron restriction prevents development of immune memory to *T. gondii*.

509 ***CD4+ T cell intrinsic CD71 is required for development of CD4+ T cell responses***
510 ***during T. gondii infection***

511 Our results demonstrate that iron is critical for CD4+ and CD8+ T cell responses
512 during *T. gondii* infection and this could be why DFP induced iron restriction results in
513 higher morbidity, mortality and cyst burdens in the CNS. However, iron restriction
514 appeared to impact CD4+ T cells more than CD8+ T cells. In addition, CD4+ T cells also
515 upregulated CD71 more than CD8+ T cells after infection, and was further increased with
516 DFP induced iron restriction. Therefore, we hypothesized that CD4+ T cell intrinsic CD71
517 was required for their activation and function. To test this hypothesis, we generated CD4-
518 $CreER^{T2}$ :: $CD71^{Flx/Flx}$ mice for tamoxifen induced conditional knockout of CD71 in CD4+
519 T cells (Figure S4).

520 CD4+ conditional CD71 knockout mice (CD4cCD71KO) were infected with ME49
521 cysts and the CD4+ and CD8+ T cell frequency and absolute numbers were measured
522 by flow cytometry. The frequency and number of total CD4+ T cells in CD4cCD71KO
523 compared to WT $CreER^{T2}$ negative littermate controls was significantly reduced (Figure
524 7A, C). Surprisingly, the total CD8+ T cell population, not non-T cell populations,

525 increased in frequency and absolute number in the CD4cCD71KO mice (Figure 7A, B,
526 D). As further validation of the model, CD71 expression was significantly reduced on the
527 CD4+ T cells in the CD4cCD71KO compared to WT littermate controls (Figure 7E). There
528 was no change in TfR1 expression in CD8+ T cells (Figure 7F). To determine why the
529 CD4+ T cell population was reduced we measured their proliferation using the
530 proliferation marker Ki67 (67). Ki67 expression was reduced in CD4+ T cells from the
531 CD4cCD71KO group by 52.7% compared to WT littermate controls (Figure 7G).

532 To examine how iron uptake via CD71 in CD4+ T cells impacted the immune
533 response to *T. gondii*, we measured antigen experience (CD11aHiCD49d+) and
534 functionality of CD4+ and CD8+ T cell subsets in CD4cCD71KO mice and WT littermate
535 controls after ME49 infection. The frequency of antigen experienced CD4+ T cells in the
536 CD4cCD71KO + tamoxifen group was 38.90%, significantly lower than the non-tamoxifen
537 treated CD4cCD71KO (57.20%) and WT littermate controls with or without tamoxifen
538 (53.56% and 58.01%, respectively) (Figure 8A). CD4+ T cells are required to maintain
539 CD8+ T cell responses and memory development (26). To our surprise, the frequency
540 and absolute number of antigen experienced CD11aHi CD49d+ CD8+ T Cells were not
541 significantly different comparing CD4cCD71KO (58.33% in untreated and 64.84% in
542 tamoxifien-treated) WT littermate controls (59.51% in untreated and 55.23% in tamoxifen-
543 treated) (Figure 8B). The frequency and absolute number of polyfunctional CD4+ T cells
544 was highly dependent on CD71 (Figure 8C). The polyfunctional (IFNγ+/TNFα+) CD4+ T
545 cell proportions were reduced to 1.13% in tamoxifen-treated CD4cCD71KO from 11.46%
546 and 6.78% in the littermate controls and 10.76% non-tamoxifen treated CD4cCD71KO
547 (Figure 8C). There was no significant difference in the functional CD8+ T cell response

548 across all groups (Figure 8D) suggesting that iron largely regulates the ability of the CD4+
549 T cells to expand and function during infection independent of CD4+ T cell help to
550 developing CD8+ T cell responses. To further test this possibility we infected all mouse
551 groups with ME49 and measured survival. No significant difference in survival was
552 observed comparing CD4cCD71KO to WT litter mate controls with or without tamoxifen
553 treatment (Figure 8E), supporting the importance of iron uptake for CD4 function, but not
554 for helping CD8+ T cell responses develop.
555

556 Discussion

557 Competition between host and pathogen for nutritional iron shapes the
558 pathogenesis and outcome of infections. Here, we investigated this complex interaction
559 during *T. gondii* infection. Our results demonstrate that iron is not only essential for
560 *Toxoplasma gondii* replication, but also for optimal host immune responses because
561 restricting iron *in vivo* results in higher morbidity and mortality in mice. During iron
562 restriction with DFP, splenic and systemic IL-12 and IFNγ levels were significantly
563 reduced in acute infection. However, in the absence of adaptive immune cells in RAG1-
564 /- mice, iron restriction does not further enhance mortality due to infection. The immune
565 cells impacted the most by iron restriction were CD4+ and CD8+ T cells, as antigen
566 experience of both and CD4+ functionality were dependent on iron. Importantly, iron
567 restriction inhibition of CD4+ and CD8+ T cells was independent of antigen load and was
568 essential for development of vaccine induced long-term protection against lethal *T. gondii*
569 challenge. Both CD4+ and CD8+ T cells upregulate CD71 protein expression in response
570 to *T. gondii*, and especially so by antigen experienced CD4+ T cells when iron is limited.
571 Lastly, we find that CD71 expression is required for expansion of antigen experienced
572 and polyfunctional CD4+ T cell in a cell intrinsic manner. Taken together, these results
573 suggest that iron homeostasis is a required nutrient for efficient CD4+ and CD8+ T cell
574 responses to *T.* gondii and regulated by CD71 in CD4+ T cells. The implications of this
575 study suggest that iron nutrition is an extenuating factor not only for resisting primary
576 infections, but with long lasting effects even after iron balance is restored for vaccine
577 efficacy.

578 The absolute requirement for iron in *T. gondii* biology remains an attractive target
579 for therapeutic intervention, however, restricting iron could also have a negative effect on
580 the development of immunity to this infection. The levels of IL-12 and IFNγ at 5DPI were
581 reduced by iron restriction in both serum and spleen, but not completely absent. IL-12 is
582 produced by the myeloid cell populations including neutrophils, monocytes, macrophages
583 and dendritic cells during *T. gondii* infection (45, 46). Iron overload can affect the
584 polarization and differentiation of monocytes into macrophages via mitochondrial
585 oxidative stress (32, 33). Treatment of iron deficiency with intravenous iron can affect the
586 differentiation of monocytes into macrophages and DCs (34). Although iron homeostasis
587 could be important in these roles, we did not observe any significant difference in the
588 ratios of these cells in the spleen during acute infection, suggesting that DFP induced iron
589 restriction may not significantly impair myeloid cell cellular composition during *T. gondii*
590 infection. IL-12-dependent IFNγ produced by NK cells is critical for early control of *T.*
591 *gondii* and reaches its peak by day 5 post infection (22). Our results reveal NK cell
592 responses in DFP induced iron restriction conditions remained intact at that time point
593 compared to normal iron conditions. These results further support that iron may not have
594 an important role in innate immunity to *T. gondii*. Taken together, this could indicate that
595 parasite detection by the innate immune system was impaired and translates to lower
596 cytokine production *in vivo,* but the potential capacity of NK cell IFNγ production is
597 independent of iron homeostasis. Further exploration of the impact of iron in innate
598 immunity to *T. gondii* is warranted to answer these questions.
599 Available iron and CD4+ T cell intrinsic CD71 are critical factors for the
600 development of adaptive immunity to *T. gondii* infection. Blockade of CD71 transporting

601 iron on human CD4+ T cells prevents their proliferation after anti-CD3/CD28 activation
602 (38). Iron status can also affect the differentiation of T helper cell type, potentially
603 impairing development of proper T helper populations important for controlling disease
604 (37, 39, 40). Our results demonstrate that iron levels do impact the development of T cell
605 responses during *T. gondii* infection. Expansion of antigen experienced CD11a(Hi)
606 CD49d+ CD4+ and CD8+ T cells and CD4+ T cell functionality were inhibited in iron
607 restriction conditions during *T. gondii* infection and after vaccination. CD4+ T cell intrinsic
608 CD71 was essential for antigen experienced cell expansion and optimal polyfunctional
609 responses. There are several possibilities that may explain the role of iron and CD71 in
610 T cell expansion and activation during *T. gondii* infection.

611 Iron levels in a T cell can be sensed and could provide post transcriptional
612 regulation of critical genes for T cell activation, proliferation, function, and differentiation.
613 Iron is a known cofactor for Iron-Responsive Element (IRE) Binding Protein 1 (IRP1),
614 which is a regulator of translation for many proteins, such as CD71, by differential binding
615 of mRNA IRE's (68). T cell transcription factors such as Tbx21, Eomesoderm, PRDM1,
616 Akt/mTor, NFκB, TCF1, and STATs, all critical for T cell activation, could contain IREs in
617 their 5' and 3' UTRs that IRP1 could then bind to regulate their expression depending on
618 cellular iron levels. There is evidence that at least Tbx21 and STAT1 may be mitigated by
619 iron levels (69, 70).

620 T cell activation requires a metabolic shift to support their activation, proliferation,
621 differentiation, and function to control diseases. Naïve, memory, and effector T cells
622 exhibit distinct metabolic profiles (71-75) and undergoing a metabolic shift once they
623 receive proper activation signals for antigen recognition, costimulation, and cytokines (76,

624 77). Iron and uptake via CD71 may supply sufficient iron levels for energetic demands of
625 T cell activation. In addition to regulating mRNA stability and translation, IRP1 also works
626 to regulate the citric acid cycle (TCA cycle) as aconitase when iron sulfur clusters are
627 bound (78). Our study may have revealed how iron uptake is a critical fourth signal to
628 turn on metabolic activity for CD4+ and CD8+ T cell expansion and function and how this
629 is also critical for vaccine efficacy against this infection. Interestingly, our results also
630 demonstrate that iron and CD71 mediated iron uptake is more important for CD4+ T cells
631 to become activated than CD8+ T cells.

632 The activation, proliferation, differentiation and function of T cells can be regulated
633 by critical second messengers: reactive oxygen species (ROS) produced inside of T cells.
634 Iron and CD71 dependent iron uptake could impact ROS levels thereby affecting their
635 intracellular signaling for activation. Iron reacts with hydrogen peroxide to produce
636 hydroxy radicals (OH) by the Fenton reaction (79). The level of ROS and hydroxy radicals
637 can be sensed by glutathione which then in turn regulates T cell proliferation (80). ROS
638 can also be detected by the Nrf2-KEAP1-Cul3 which releases Nrf2 from the complex to
639 become an active suppressor of T cell activation (80). Maintenance of moderate levels of
640 ROS is also essential for proper TCR signaling that then can enhance T cell activation,
641 proliferation, differentiation, and function (81-84). Understanding how iron and CD71
642 uptake impacts ROS signaling in T cells during *T. gondii* infection will be important future
643 research.

644 CD71 may function independently of iron uptake in T cell activation. CD71 has
645 been observed to co-localize with the T Cell Receptor (TCR) complex and to be a
646 functional signaling component of the immune synapse (85). The mechanism(s) of how

647 CD71 interacting with the TCR complex influence the level of T cell activation are
648 unknown. CD71 is phosphorylated by Protein Kinase C (PKC) at position serine 24 in the
649 cytoplasmic domain of CD71 away from the transferrin binding site (86, 87). Endocytosis
650 of CD71 is required for iron uptake, but the serine 24 residue is dispensable for it,
651 suggesting a potential still-undiscovered function of CD71 phosphorylation (88-90). Since
652 PKC is central to TCR engagement downstream of CD3 and CD28 signaling (91),
653 phosphorylation of CD71 by PKC would spatiotemporally position CD71 to contribute to
654 signaling as part of the TCR complex. CD71 expression is ultimately controlled by IRP1-
655 dependent iron sensing, therefore the secondary potential signaling function of CD71 in
656 the TCR could act as another checkpoint for adequate iron levels to support T cell
657 activation.

658 CD4+ and CD8+ T cells' reliance on iron was different depending on strain of *T.*
659 *gondii* infection. Our results indicate that iron may be more essential for regulating CD4+
660 T cell effector responses than CD8+ T cell effector responses during Type II *T. gondii*
661 strain acute infection, but that effector responses of both CD4+ and CD8+ T cells are
662 equally reliant on available iron after vaccination with the attenuated vaccine strain CPS.
663 Antigen processing *T. gondii* infection can occur through cross presentation,
664 phagocytosis, or autophagy (92-94). In typical type II ME49 infections, proliferation of the
665 parasite is coupled with antigen processing, but in DFP induced iron limiting conditions,
666 the parasite proliferation and dissemination are altered. This may differentially affect
667 modes of antigen processing and presentation to CD4+ T cells compared to CD8+ T cells.
668 For example, since iron levels influence autophagic potential of cells (95) and autophagy
669 is a major route for MHCII antigen processing (96), it is plausible that modulation of

670 autophagy by iron restriction preferentially inhibits antigen processing important for
671 antigen experience for both CD4+ and CD8+ T cells but inhibits function of only CD4+ T
672 cells in ME49 studies. In contrast, in CPS vaccination studies, the parasite cannot
673 proliferate, thus, the potential differing effects of iron restriction on antigen processing and
674 presentation to CD4+ or CD8+ T cells would be equal, providing some explanation as to
675 why we observed inhibition of both CD4+ and CD8+ T cells in terms of antigen experience
676 and function. Additionally, in both CPS and ME49 strain infections, the proportion of CD8+
677 FIII and FIV effector subpopulations, not the FII memory precursor subpopulation, were
678 inhibited by iron restriction, suggesting that the type and strength of the CD8+ T cell
679 response relies on iron as much as CD4+ T cell polyfunctional response.

680 In addition, CD4+ T cells may be more reliant on iron uptake by CD71 than CD8+
681 T cells. Our data may support this possibility because we observed that only antigen
682 experienced CD4+ T cells upregulated their CD71 to a higher level in iron limiting
683 conditions with DFP. CD4+ T cells are required to provide help for the activation,
684 maintenance of activation, and memory cell differentiation of CD8+ T cells during *T. gondii*
685 infection (24, 26, 66). The conditional knockout of CD71 in CD4+ T cells reduced overall
686 frequencies and number of CD4+ T cells, CD4+ T cell antigen experience, and CD4+
687 functionality. These results demonstrate that CD71 is critical for development of CD4+ T
688 cell responses to *T. gondii*. Based on these results we were expecting that there would
689 be a decrease in CD8+ T cell responses due to the lack of CD4+ T cell help in the absence
690 of CD71. However, this was not the case; within the CD8+ T cell compartment, there was
691 no change of antigen experience or functionality in the CD4cCD71KO mouse treated with
692 tamoxifen compared to all other groups. Intriguingly, the reduced frequency of total CD4+

693 T cells in the spleen in the CD4cCD71KO mice treated with tamoxifen was compensated
694 by an increase in total CD8+ T cell frequencies and numbers. It is possible that the
695 compensatory increase of overall CD8+ numbers could additionally compensate for
696 reduced protection provided by CD4+ T cells in the conditional knockout, resulting in
697 similar disease outcomes. A recent study has demonstrated that CD71 antibody blockade
698 that inhibits iron uptake by human CD4+ T cells still results in generation of accessory
699 helper T cells *in vitro* (38). An alternative explanation for our results then is that by
700 knocking down expression of CD71 in CD4+ T cells, the generation of these accessory
701 CD4+ T cell helper cells is retained. While overall functionality and expansion of antigen
702 experienced CD4+ T cells is reduced, these cells might provide CD8+ T cells with the
703 help they need to continue to function and develop memory. This is further supported by
704 our survival data that shows no difference in long-term survival between CD4cCD71KO
705 tamoxifen treated and WT litter mate controls. Further studies of the role of CD71 in the
706 T cell responses to *T. gondii*, whether iron-dependent or -independent, will be helpful to
707 uncover additional roles for iron as a fourth signal regulating T cell immunity during this
708 infection.

709 In summary, the results of this study confirm the nutritional requirement of iron for
710 both *Toxoplasma gondii* and its corresponding immune response and defined the adverse
711 outcome of mice that do not meet this nutritional need. The mechanism driving the
712 adverse outcome is explained by defective CD4+ and CD8+ T cell responses. Optimal
713 CD4+ T cells responses were mediated by iron uptake receptor Transferrin Receptor 1.
714 Many questions remain and will be addressed in future studies.

715 Acknowledgements

716 The principal investigator and corresponding author of this project is J.P.G. Project
717 conception was conducted by S.L.D. and J.P.G. Experiments were designed by S.L.D.
718 and performed by S.L.D., T.R., M.A., H.K.K., and S.K.N. Data analysis was conducted by
719 S.L.D., T.R., and M.A. Intellectual contributions were made by S.L.D. and J.P.G.
720 Technical expertise was provided by J.P.G. Manuscript preparation was performed by
721 S.L.D. and J.P.G., with contributions by all authors on revisions. Funding securement and
722 project management was performed by J.P.G.

723 References

724 1. Pappas, G., N. Roussos, and M. E. Falagas. 2009. Toxoplasmosis snapshots:
725 global status of Toxoplasma gondii seroprevalence and implications for pregnancy
726 and congenital toxoplasmosis. *International journal for parasitology* 39: 1385-
727 1394.
728 2. Luft, B. J., and J. S. Remington. 1988. AIDS commentary. Toxoplasmic
729 encephalitis. *The Journal of infectious diseases* 157: 1-6.
730 3. Tenter, A. M., A. R. Heckeroth, and L. M. Weiss. 2000. Toxoplasma gondii: from
731 animals to humans. *International journal for parasitology* 30: 1217-1258.
732 4. Fox, B. A., J. P. Gigley, and D. J. Bzik. 2004. Toxoplasma gondii lacks the enzymes
733 required for de novo arginine biosynthesis and arginine starvation triggers cyst
734 formation. *International journal for parasitology* 34: 323-331.
735 5. Krug, E. C., J. J. Marr, and R. L. Berens. 1989. Purine metabolism in Toxoplasma
736 gondii. *J Biol Chem* 264: 10601-10607.
737 6. Romano, J. D., S. Sonda, E. Bergbower, M. E. Smith, and I. Coppens. 2013.
738 Toxoplasma gondii salvages sphingolipids from the host Golgi through the

739 rerouting of selected Rab vesicles to the parasitophorous vacuole. *Mol Biol Cell*
740 24: 1974-1995.
741 7. Ma, E. H., G. Bantug, T. Griss, S. Condotta, R. M. Johnson, B. Samborska, N.
742 Mainolfi, V. Suri, H. Guak, M. L. Balmer, M. J. Verway, T. C. Raissi, H. Tsui, G.
743 Boukhaled, S. Henriques da Costa, C. Frezza, C. M. Krawczyk, A. Friedman, M.
744 Manfredi, M. J. Richer, C. Hess, and R. G. Jones. 2017. Serine Is an Essential
745 Metabolite for Effector T Cell Expansion. *Cell metabolism* 25: 345-357.
746 8. Tanaka, Y., Y. Nagai, M. Okumura, M. I. Greene, and T. Kambayashi. 2020.
747 PRMT5 Is Required for T Cell Survival and Proliferation by Maintaining Cytokine
748 Signaling. *Front Immunol* 11: 621.
749 9. Nagafuku, M., K. Okuyama, Y. Onimaru, A. Suzuki, Y. Odagiri, T. Yamashita, K.
750 Iwasaki, M. Fujiwara, M. Takayanagi, I. Ohno, and J. Inokuchi. 2012. CD4 and
751 CD8 T cells require different membrane gangliosides for activation. *Proceedings*
752 *of the National Academy of Sciences of the United States of America* 109: E336-
753 342.
754 10. Aghabi, D., M. Sloan, Z. Dou, A. J. Guerra, and C. R. Harding. 2021. The vacuolar
755 iron transporter mediates iron detoxification in Toxoplasma gondii. *bioRxiv*.
756 11. Almeida, M. P. O., E. A. V. Ferro, M. P. P. Briceño, M. C. Oliveira, B. F. Barbosa,
757 and N. M. Silva. 2019. Susceptibility of human villous (BeWo) and extravillous
758 (HTR-8/SVneo) trophoblast cells to Toxoplasma gondii infection is modulated by
759 intracellular iron availability. *Parasitol Res* 118: 1559-1572.

760 12. Dimier, I. H., and D. T. Bout. 1998. Interferon-gamma-activated primary
761 enterocytes inhibit Toxoplasma gondii replication: a role for intracellular iron.
762 *Immunology* 94: 488-495.
763 13. Byrd, T. F., and M. A. Horwitz. 1993. Regulation of transferrin receptor expression
764 and ferritin content in human mononuclear phagocytes. Coordinate upregulation
765 by iron transferrin and downregulation by interferon gamma. *The Journal of clinical*
766 *investigation* 91: 969-976.
767 14. Gail, M., U. Gross, and W. Bohne. 2004. Transferrin receptor induction in
768 Toxoplasma gondii-infected HFF is associated with increased iron-responsive
769 protein 1 activity and is mediated by secreted factors. *Parasitol Res* 94: 233-239.
770 15. Oliveira, M. C., L. B. Coutinho, M. P. O. Almeida, M. P. Briceno, E. C. B. Araujo,
771 and N. M. Silva. 2020. The Availability of Iron Is Involved in the Murine
772 Experimental Toxoplasma gondii Infection Outcome. *Microorganisms* 8.
773 16. Plattner, F., F. Yarovinsky, S. Romero, D. Didry, M. F. Carlier, A. Sher, and D.
774 Soldati-Favre. 2008. Toxoplasma profilin is essential for host cell invasion and
775 TLR11-dependent induction of an interleukin-12 response. *Cell host & microbe* 3:
776 77-87.
777 17. Yarovinsky, F., S. Hieny, and A. Sher. 2008. Recognition of Toxoplasma gondii by
778 TLR11 prevents parasite-induced immunopathology. *Journal of immunology*
779 *(Baltimore, Md. : 1950)* 181: 8478-8484.
780 18. Gazzinelli, R. T., M. Wysocka, S. Hayashi, E. Y. Denkers, S. Hieny, P. Caspar, G.
781 Trinchieri, and A. Sher. 1994. Parasite-induced IL-12 stimulates early IFN-gamma

782 synthesis and resistance during acute infection with Toxoplasma gondii. *Journal*
783 *of immunology (Baltimore, Md. : 1950)* 153: 2533-2543.
784 19. Chen, M., F. Aosai, K. Norose, H. S. Mun, O. Takeuchi, S. Akira, and A. Yano.
785 2002. Involvement of MyD88 in host defense and the down-regulation of anti-heat
786 shock protein 70 autoantibody formation by MyD88 in Toxoplasma gondii-infected
787 mice. *The Journal of parasitology* 88: 1017-1019.
788 20. Hitziger, N., I. Dellacasa, B. Albiger, and A. Barragan. 2005. Dissemination of
789 Toxoplasma gondii to immunoprivileged organs and role of Toll/interleukin-1
790 receptor signalling for host resistance assessed by in vivo bioluminescence
791 imaging. *Cell Microbiol* 7: 837-848.
792 21. Hunter, C. A., C. S. Subauste, V. H. Van Cleave, and J. S. Remington. 1994.
793 Production of gamma interferon by natural killer cells from Toxoplasma gondii-
794 infected SCID mice: regulation by interleukin-10, interleukin-12, and tumor
795 necrosis factor alpha. *Infection and immunity* 62: 2818-2824.
796 22. Gazzinelli, R. T., S. Hieny, T. A. Wynn, S. Wolf, and A. Sher. 1993. Interleukin 12
797 is required for the T-lymphocyte-independent induction of interferon gamma by an
798 intracellular parasite and induces resistance in T-cell-deficient hosts. *Proceedings*
799 *of the National Academy of Sciences of the United States of America* 90: 6115-
800 6119.
801 23. López-Yglesias, A. H., E. Burger, E. Camanzo, A. T. Martin, A. M. Araujo, S. F.
802 Kwok, and F. Yarovinsky. 2021. T-bet-dependent ILC1- and NK cell-derived IFN-
803 γ mediates cDC1-dependent host resistance against Toxoplasma gondii. *PLoS*
804 *pathogens* 17: e1008299.

805 24. Gigley, J. P., B. A. Fox, and D. J. Bzik. 2009. Cell-mediated immunity to
806 Toxoplasma gondii develops primarily by local Th1 host immune responses in the
807 absence of parasite replication. *Journal of immunology (Baltimore, Md. : 1950)*
808 182: 1069-1078.
809 25. Gigley, J. P., B. A. Fox, and D. J. Bzik. 2009. Long-term immunity to lethal acute
810 or chronic type II Toxoplasma gondii infection is effectively induced in genetically
811 susceptible C57BL/6 mice by immunization with an attenuated type I vaccine
812 strain. *Infection and immunity* 77: 5380-5388.
813 26. Casciotti, L., K. H. Ely, M. E. Williams, and I. A. Khan. 2002. CD8(+)-T-cell
814 immunity against Toxoplasma gondii can be induced but not maintained in mice
815 lacking conventional CD4(+) T cells. *Infection and immunity* 70: 434-443.
816 27. Bhadra, R., J. P. Gigley, L. M. Weiss, and I. A. Khan. 2011. Control of Toxoplasma
817 reactivation by rescue of dysfunctional CD8+ T-cell response via PD-1-PDL-1
818 blockade. *Proceedings of the National Academy of Sciences of the United States*
819 *of America* 108: 9196-9201.
820 28. Ivanova, D. L., R. Krempels, S. L. Denton, K. D. Fettel, G. M. Saltz, D. Rach, R.
821 Fatima, T. Mundhenke, J. Materi, I. R. Dunay, and J. P. Gigley. 2020. NK Cells
822 Negatively Regulate CD8 T Cells to Promote Immune Exhaustion and Chronic
823 Toxoplasma gondii Infection. *Frontiers in cellular and infection microbiology* 10:
824 313.
825 29. Xiao, J., Y. Li, R. H. Yolken, and R. P. Viscidi. 2018. PD-1 immune checkpoint
826 blockade promotes brain leukocyte infiltration and diminishes cyst burden in a
827 mouse model of Toxoplasma infection. *Journal of neuroimmunology* 319: 55-62.

828 30. Hwang, S., D. A. Cobb, R. Bhadra, B. Youngblood, and I. A. Khan. 2016. Blimp-1-
829 mediated CD4 T cell exhaustion causes CD8 T cell dysfunction during chronic
830 toxoplasmosis. *The Journal of experimental medicine* 213: 1799-1818.
831 31. Kono, M., S. Matsuhiroya, A. Obuchi, T. Takahashi, S. Imoto, S. Kawano, and K.
832 Saigo. 2020. Deferasirox, an iron-chelating agent, alleviates acute lung
833 inflammation by inhibiting neutrophil activation and extracellular trap formation. *J*
834 *Int Med Res* 48: 300060520951015.
835 32. Agoro, R., M. Taleb, V. F. J. Quesniaux, and C. Mura. 2018. Cell iron status
836 influences macrophage polarization. *PloS one* 13: e0196921.
837 33. Cui, Y., S. Gutierrez, S. Ariai, L. Öberg, K. Thörn, U. Gehrmann, S. M. Cloonan, T.
838 Naessens, and H. Olsson. 2022. Non-heme iron overload impairs monocyte to
839 macrophage differentiation via mitochondrial oxidative stress. *Frontiers in*
840 *Immunology* 13.
841 34. Fell, L. H., S. Seiler-Mussler, A. B. Sellier, B. Rotter, P. Winter, M. Sester, D. Fliser,
842 G. H. Heine, and A. M. Zawada. 2016. Impact of individual intravenous iron
843 preparations on the differentiation of monocytes towards macrophages and
844 dendritic cells. *Nephrol Dial Transplant* 31: 1835-1845.
845 35. Flynn, M. G., L. Mackinnon, V. Gedge, M. Fahlman, and T. Brickman. 2003.
846 Influence of iron status and iron supplements on natural killer cell activity in trained
847 women runners. *Int J Sports Med* 24: 217-222.
848 36. Baines, M. G., F. L. Lafleur, and B. E. Holbein. 1983. Involvement of transferrin
849 and transferrin receptors in human natural killer effector:target interaction.
850 *Immunol Lett* 7: 51-55.

851 37. Yarosz, E. L., C. Ye, A. Kumar, C. Black, E. K. Choi, Y. A. Seo, and C. H. Chang.
852 2020. Cutting Edge: Activation-Induced Iron Flux Controls CD4 T Cell Proliferation
853 by Promoting Proper IL-2R Signaling and Mitochondrial Function. *Journal of*
854 *immunology (Baltimore, Md. : 1950)* 204: 1708-1713.
855 38. Berg, V., M. Modak, J. Brell, A. Puck, S. Kunig, S. Jutz, P. Steinberger, G. J.
856 Zlabinger, and J. Stockl. 2020. Iron Deprivation in Human T Cells Induces
857 Nonproliferating Accessory Helper Cells. *Immunohorizons* 4: 165-177.
858 39. Pfeifhofer-Obermair, C., P. Tymoszuk, M. Nairz, A. Schroll, G. Klais, E. Demetz,
859 S. Engl, N. Brigo, and G. Weiss. 2021. Regulation of Th1 T Cell Differentiation by
860 Iron via Upregulation of T Cell Immunoglobulin and Mucin Containing Protein-3
861 (TIM-3). *Front Immunol* 12: 637809.
862 40. Leung, S., A. Holbrook, B. King, H. T. Lu, V. Evans, N. Miyamoto, C. Mallari, S.
863 Harvey, D. Davey, E. Ho, W. W. Li, J. Parkinson, R. Horuk, S. Jaroch, M. Berger,
864 W. Skuballa, C. West, R. Pulk, G. Phillips, J. Bryant, B. Subramanyam, C.
865 Schaefer, H. Salamon, E. Lyons, D. Schilling, H. Seidel, J. Kraetzschmar, M.
866 Snider, and D. Perez. 2005. Differential inhibition of inducible T cell cytokine
867 secretion by potent iron chelators. *J Biomol Screen* 10: 157-167.
868 41. Rodriguez, R., C. L. Jung, V. Gabayan, J. C. Deng, T. Ganz, E. Nemeth, and Y.
869 Bulut. 2014. Hepcidin induction by pathogens and pathogen-derived molecules is
870 strongly dependent on interleukin-6. *Infection and immunity* 82: 745-752.
871 42. Chen, A. C., A. Donovan, R. Ned-Sykes, and N. C. Andrews. 2015. Noncanonical
872 role of transferrin receptor 1 is essential for intestinal homeostasis. *Proceedings of*

873 *the National Academy of Sciences of the United States of America* 112: 11714-
874 11719.
875 43. Hatcher, H. C., R. N. Singh, F. M. Torti, and S. V. Torti. 2009. Synthetic and natural
876 iron chelators: therapeutic potential and clinical use. *Future Med Chem* 1: 1643-
877 1670.
878 44. Adams, L. B., J. B. Hibbs, Jr., R. R. Taintor, and J. L. Krahenbuhl. 1990.
879 Microbiostatic effect of murine-activated macrophages for Toxoplasma gondii.
880 Role for synthesis of inorganic nitrogen oxides from L-arginine. *Journal of*
881 *immunology (Baltimore, Md. : 1950)* 144: 2725-2729.
882 45. Liu, C.-H., Y.-t. Fan, A. Dias, L. Esper, R. A. Corn, A. Bafica, F. S. Machado, and
883 J. Aliberti. 2006. Cutting Edge: Dendritic Cells Are Essential for In Vivo IL-12
884 Production and Development of Resistance against Toxoplasma gondii Infection
885 in Mice. *The Journal of Immunology* 177: 31-35.
886 46. Mercer, H. L., L. M. Snyder, C. M. Doherty, B. A. Fox, D. J. Bzik, and E. Y. Denkers.
887 2020. Toxoplasma gondii dense granule protein GRA24 drives MyD88-
888 independent p38 MAPK activation, IL-12 production and induction of protective
889 immunity. *PLoS pathogens* 16: e1008572.
890 47. Mombaerts, P., J. Iacomini, R. S. Johnson, K. Herrup, S. Tonegawa, and V. E.
891 Papaioannou. 1992. RAG-1-deficient mice have no mature B and T lymphocytes.
892 *Cell* 68: 869-877.
893 48. Hunter, C. A., R. Chizzonite, and J. S. Remington. 1995. Il-1-Beta Is Required for
894 Il-12 to Induce Production of Ifn-Gamma by Nk-Cells - a Role for Il-1-Beta in the T-

895 Cell-Independent Mechanism of Resistance against Intracellular Pathogens.
896 *Journal of Immunology* 155: 4347-4354.
897 49. Goldszmid, R. S., P. Caspar, A. Rivollier, S. White, A. Dzutsev, S. Hieny, B. Kelsall,
898 G. Trinchieri, and A. Sher. 2012. NK cell-derived interferon-gamma orchestrates
899 cellular dynamics and the differentiation of monocytes into dendritic cells at the site
900 of infection. *Immunity* 36: 1047-1059.
901 50. Lee, Y. H., J. Y. Channon, T. Matsuura, J. D. Schwartzman, D. W. Shin, and L. H.
902 Kasper. 1999. Functional and quantitative analysis of splenic T cell immune
903 responses following oral toxoplasma gondii infection in mice. *Experimental*
904 *parasitology* 91: 212-221.
905 51. Carrof, B., M. Levacher-Clergeot, F. Chau, J. J. Pocidalo, and F. Derouin. 1994.
906 Toxoplasma gondii: kinetics of lymphocyte subsets in blood and spleen of perorally
907 infected mice. *Experimental parasitology* 78: 410-417.
908 52. McDermott, D. S., and S. M. Varga. 2011. Quantifying antigen-specific CD4 T cells
909 during a viral infection: CD4 T cell responses are larger than we think. *Journal of*
910 *immunology (Baltimore, Md. : 1950)* 187: 5568-5576.
911 53. Haque, S., J. Franck, H. Dumon, L. H. Kasper, and A. Haque. 1999. Protection
912 against lethal toxoplasmosis in mice by an avirulent strain of Toxoplasma gondii:
913 stimulation of IFN-gamma and TNF-alpha response. *Experimental parasitology* 93:
914 231-240.
915 54. Gazzinelli, R. T., I. Eltoum, T. A. Wynn, and A. Sher. 1993. Acute cerebral
916 toxoplasmosis is induced by in vivo neutralization of TNF-alpha and correlates with
917 the down-regulated expression of inducible nitric oxide synthase and other

918 markers of macrophage activation. *Journal of immunology (Baltimore, Md. : 1950)*
919 151: 3672-3681.
920 55. Shirahata, T., T. Yamashita, C. Ohta, H. Goto, and A. Nakane. 1994. CD8+ T
921 lymphocytes are the major cell population involved in the early gamma interferon
922 response and resistance to acute primary Toxoplasma gondii infection in mice.
923 *Microbiol Immunol* 38: 789-796.
924 56. Jongert, E., A. Lemiere, J. Van Ginderachter, S. De Craeye, K. Huygen, and S.
925 D'Souza. 2010. Functional characterization of in vivo effector CD4(+) and CD8(+)
926 T cell responses in acute Toxoplasmosis: an interplay of IFN-gamma and cytolytic
927 T cells. *Vaccine* 28: 2556-2564.
928 57. Denkers, E. Y., and R. T. Gazzinelli. 1998. Regulation and function of T-cell-
929 mediated immunity during Toxoplasma gondii infection. *Clinical microbiology*
930 *reviews* 11: 569-588.
931 58. Giannetti, A. M., P. J. Halbrooks, A. B. Mason, T. M. Vogt, C. A. Enns, and P. J.
932 Bjorkman. 2005. The molecular mechanism for receptor-stimulated iron release
933 from the plasma iron transport protein transferrin. *Structure* 13: 1613-1623.
934 59. Bayer, A. L., P. Baliga, and J. E. Woodward. 1998. Transferrin receptor in T cell
935 activation and transplantation. *Journal of leukocyte biology* 64: 19-24.
936 60. Brekelmans, P., P. van Soest, P. J. Leenen, and W. van Ewijk. 1994. Inhibition of
937 proliferation and differentiation during early T cell development by anti-transferrin
938 receptor antibody. *European journal of immunology* 24: 2896-2902.

939 61. Brekelmans, P., P. van Soest, J. Voerman, P. P. Platenburg, P. J. Leenen, and W.
940 van Ewijk. 1994. Transferrin receptor expression as a marker of immature cycling
941 thymocytes in the mouse. *Cellular immunology* 159: 331-339.
942 62. Wilson, D. C., S. Matthews, and G. S. Yap. 2008. IL-12 signaling drives CD8+ T
943 cell IFN-gamma production and differentiation of KLRG1+ effector subpopulations
944 during Toxoplasma gondii Infection. *Journal of immunology (Baltimore, Md. : 1950)*
945 180: 5935-5945.
946 63. Sanecka, A., N. Yoshida, E. M. Kolawole, H. Patel, B. D. Evavold, and E. M.
947 Frickel. 2018. T Cell Receptor-Major Histocompatibility Complex Interaction
948 Strength Defines Trafficking and CD103(+) Memory Status of CD8 T Cells in the
949 Brain. *Front Immunol* 9: 1290.
950 64. Moretto, M. M., J. Chen, M. Meador, J. Phan, and I. A. Khan. 2023. A Lower Dose
951 of Infection Generates a Better Long-Term Immune Response against
952 Toxoplasma gondii. *Immunohorizons* 7: 177-190.
953 65. Fox, B. A., and D. J. Bzik. 2002. De novo pyrimidine biosynthesis is required for
954 virulence of Toxoplasma gondii. *Nature* 415: 926-929.
955 66. Jordan, K. A., E. H. Wilson, E. D. Tait, B. A. Fox, D. S. Roos, D. J. Bzik, F.
956 Dzierszinski, and C. A. Hunter. 2009. Kinetics and phenotype of vaccine-induced
957 CD8+ T-cell responses to Toxoplasma gondii. *Infection and immunity* 77: 3894-
958 3901.
959 67. Gerdes, J., H. Lemke, H. Baisch, H. H. Wacker, U. Schwab, and H. Stein. 1984.
960 Cell cycle analysis of a cell proliferation-associated human nuclear antigen defined

961 by the monoclonal antibody Ki-67. *Journal of immunology (Baltimore, Md. : 1950)*
962 133: 1710-1715.
963 68. Hentze, M. W., and L. C. Kuhn. 1996. Molecular control of vertebrate iron
964 metabolism: mRNA-based regulatory circuits operated by iron, nitric oxide, and
965 oxidative stress. *Proceedings of the National Academy of Sciences of the United*
966 *States of America* 93: 8175-8182.
967 69. Van Den Ham, K. M., M. T. Shio, A. Rainone, S. Fournier, C. M. Krawczyk, and M.
968 Olivier. 2015. Iron prevents the development of experimental cerebral malaria by
969 attenuating CXCR3-mediated T cell chemotaxis. *PloS one* 10: e0118451.
970 70. Regis, G., M. Bosticardo, L. Conti, S. De Angelis, D. Boselli, B. Tomaino, P.
971 Bernabei, M. Giovarelli, and F. Novelli. 2005. Iron regulates T-lymphocyte
972 sensitivity to the IFN-gamma/STAT1 signaling pathway in vitro and in vivo. *Blood*
973 105: 3214-3221.
974 71. Rathmell, J. C., M. G. Vander Heiden, M. H. Harris, K. A. Frauwirth, and C. B.
975 Thompson. 2000. In the absence of extrinsic signals, nutrient utilization by
976 lymphocytes is insufficient to maintain either cell size or viability. *Mol Cell* 6: 683-
977 692.
978 72. Frauwirth, K. A., J. L. Riley, M. H. Harris, R. V. Parry, J. C. Rathmell, D. R. Plas,
979 R. L. Elstrom, C. H. June, and C. B. Thompson. 2002. The CD28 signaling pathway
980 regulates glucose metabolism. *Immunity* 16: 769-777.
981 73. Verbist, K. C., C. S. Guy, S. Milasta, S. Liedmann, M. M. Kaminski, R. Wang, and
982 D. R. Green. 2016. Metabolic maintenance of cell asymmetry following division in
983 activated T lymphocytes. *Nature* 532: 389-393.

984 74. Menk, A. V., N. E. Scharping, R. S. Moreci, X. Zeng, C. Guy, S. Salvatore, H. Bae,
985 J. Xie, H. A. Young, S. G. Wendell, and G. M. Delgoffe. 2018. Early TCR Signaling
986 Induces Rapid Aerobic Glycolysis Enabling Distinct Acute T Cell Effector
987 Functions. *Cell Rep* 22: 1509-1521.
988 75. Loschinski, R., M. Bottcher, A. Stoll, H. Bruns, A. Mackensen, and D.
989 Mougiakakos. 2018. IL-21 modulates memory and exhaustion phenotype of T-
990 cells in a fatty acid oxidation-dependent manner. *Oncotarget* 9: 13125-13138.
991 76. Wang, R., Christopher P. Dillon, Lewis Z. Shi, S. Milasta, R. Carter, D. Finkelstein,
992 Laura L. McCormick, P. Fitzgerald, H. Chi, J. Munger, and Douglas R. Green.
993 2011. The Transcription Factor Myc Controls Metabolic Reprogramming upon T
994 Lymphocyte Activation. *Immunity* 35: 871-882.
995 77. Frauwirth, K. A., J. L. Riley, M. H. Harris, R. V. Parry, J. C. Rathmell, D. R. Plas,
996 R. L. Elstrom, C. H. June, and C. B. Thompson. 2002. The CD28 Signaling
997 Pathway Regulates Glucose Metabolism. *Immunity* 16: 769-777.
998 78. Gray, N. K., S. Quick, B. Goossen, A. Constable, H. Hirling, L. C. Kühn, and M. W.
999 Hentze. 1993. Recombinant iron-regulatory factor functions as an iron-responsive-
1000 element-binding protein, a translational repressor and an aconitase. A functional
1001 assay for translational repression and direct demonstration of the iron switch. *Eur*
1002 *J Biochem* 218: 657-667.
1003 79. Silva-Gomes, S., S. Vale-Costa, R. Appelberg, and M. S. Gomes. 2013. Iron in
1004 intracellular infection: to provide or to deprive? *Frontiers in cellular and infection*
1005 *microbiology* 3: 96.

1006 80. Yarosz, E. L., and C. H. Chang. 2018. The Role of Reactive Oxygen Species in
1007 Regulating T Cell-mediated Immunity and Disease. *Immune Netw* 18: e14.
1008 81. Sena, L. A., S. Li, A. Jairaman, M. Prakriya, T. Ezponda, D. A. Hildeman, C.-R.
1009 Wang, P. T. Schumacker, J. D. Licht, and H. Perlman. 2013. Mitochondria are
1010 required for antigen-specific T cell activation through reactive oxygen species
1011 signaling. *Immunity* 38: 225-236.
1012 82. Lepez, A., T. Pirnay, S. Denanglaire, D. Perez-Morga, M. Vermeersch, O. Leo, and
1013 F. Andris. 2020. Long-term T cell fitness and proliferation is driven by AMPK-
1014 dependent regulation of reactive oxygen species. *Sci Rep* 10: 21673.
1015 83. Kaminski, M. M., S. W. Sauer, C. D. Klemke, D. Süss, J. G. Okun, P. H. Krammer,
1016 and K. Gülow. 2010. Mitochondrial reactive oxygen species control T cell activation
1017 by regulating IL-2 and IL-4 expression: mechanism of ciprofloxacin-mediated
1018 immunosuppression. *Journal of immunology (Baltimore, Md. : 1950)* 184: 4827-
1019 4841.
1020 84. Arbore, G., E. E. West, R. Spolski, A. A. B. Robertson, A. Klos, C. Rheinheimer,
1021 P. Dutow, T. M. Woodruff, Z. X. Yu, L. A. O'Neill, R. C. Coll, A. Sher, W. J. Leonard,
1022 J. Köhl, P. Monk, M. A. Cooper, M. Arno, B. Afzali, H. J. Lachmann, A. P. Cope,
1023 K. D. Mayer-Barber, and C. Kemper. 2016. T helper 1 immunity requires
1024 complement-driven NLRP3 inflammasome activity in $CD4^+$ T cells. *Science* 352:
1025 aad1210.
1026 85. Salmeron, A., A. Borroto, M. Fresno, M. J. Crumpton, S. C. Ley, and B. Alarcon.
1027 1995. Transferrin receptor induces tyrosine phosphorylation in T cells and is

1028 physically associated with the TCR zeta-chain. *Journal of immunology (Baltimore,*
1029 *Md. : 1950)* 154: 1675-1683.
1030 86. Davis, R. J., G. L. Johnson, D. J. Kelleher, J. K. Anderson, J. E. Mole, and M. P.
1031 Czech. 1986. Identification of serine 24 as the unique site on the transferrin
1032 receptor phosphorylated by protein kinase C. *J Biol Chem* 261: 9034-9041.
1033 87. Cheng, Y., O. Zak, P. Aisen, S. C. Harrison, and T. Walz. 2004. Structure of the
1034 human transferrin receptor-transferrin complex. *Cell* 116: 565-576.
1035 88. Rothenberger, S., B. J. Iacopetta, and L. C. Kuhn. 1987. Endocytosis of the
1036 transferrin receptor requires the cytoplasmic domain but not its phosphorylation
1037 site. *Cell* 49: 423-431.
1038 89. Zerial, M., M. Suomalainen, M. Zanetti-Schneider, C. Schneider, and H. Garoff.
1039 1987. Phosphorylation of the human transferrin receptor by protein kinase C is not
1040 required for endocytosis and recycling in mouse 3T3 cells. *The EMBO journal* 6:
1041 2661-2667.
1042 90. Davis, R. J., and H. Meisner. 1987. Regulation of transferrin receptor cycling by
1043 protein kinase C is independent of receptor phosphorylation at serine 24 in Swiss
1044 3T3 fibroblasts. *J Biol Chem* 262: 16041-16047.
1045 91. Isakov, N., and A. Altman. 2002. Protein kinase C(theta) in T cell activation. *Annu*
1046 *Rev Immunol* 20: 761-794.
1047 92. Goldszmid, R. S., I. Coppens, A. Lev, P. Caspar, I. Mellman, and A. Sher. 2009.
1048 Host ER-parasitophorous vacuole interaction provides a route of entry for antigen
1049 cross-presentation in Toxoplasma gondii-infected dendritic cells. *The Journal of*
1050 *experimental medicine* 206: 399-410.

1051 93. Lee, Y., M. Sasai, J. S. Ma, N. Sakaguchi, J. Ohshima, H. Bando, T. Saitoh, S.
1052 Akira, and M. Yamamoto. 2015. p62 Plays a Specific Role in Interferon-γ-Induced
1053 Presentation of a Toxoplasma Vacuolar Antigen. *Cell Rep* 13: 223-233.
1054 94. Yano, A., S. Ohno, K. Norose, T. Baba, K. Yamashita, F. Aosai, and K. Segawa.
1055 1992. Antigen presentation by Toxoplasma-infected cells: antigen entry through
1056 cell membrane fusion. *Int Arch Allergy Immunol* 98: 13-17.
1057 95. Wang, Y., M. Wang, Y. Liu, H. Tao, S. Banerjee, S. Srinivasan, E. Nemeth, M. J.
1058 Czaja, and P. He. 2022. Integrated regulation of stress responses, autophagy and
1059 survival by altered intracellular iron stores. *Redox Biol* 55: 102407.
1060 96. Romao, S., N. Gasser, A. C. Becker, B. Guhl, M. Bajagic, D. Vanoaica, U. Ziegler,
1061 J. Roesler, J. Dengjel, and J. Reichenbach. 2013. Autophagy proteins stabilize
1062 pathogen-containing phagosomes for prolonged MHC II antigen processing.
1063 *Journal of Cell Biology* 203: 757-766.
1064
1065

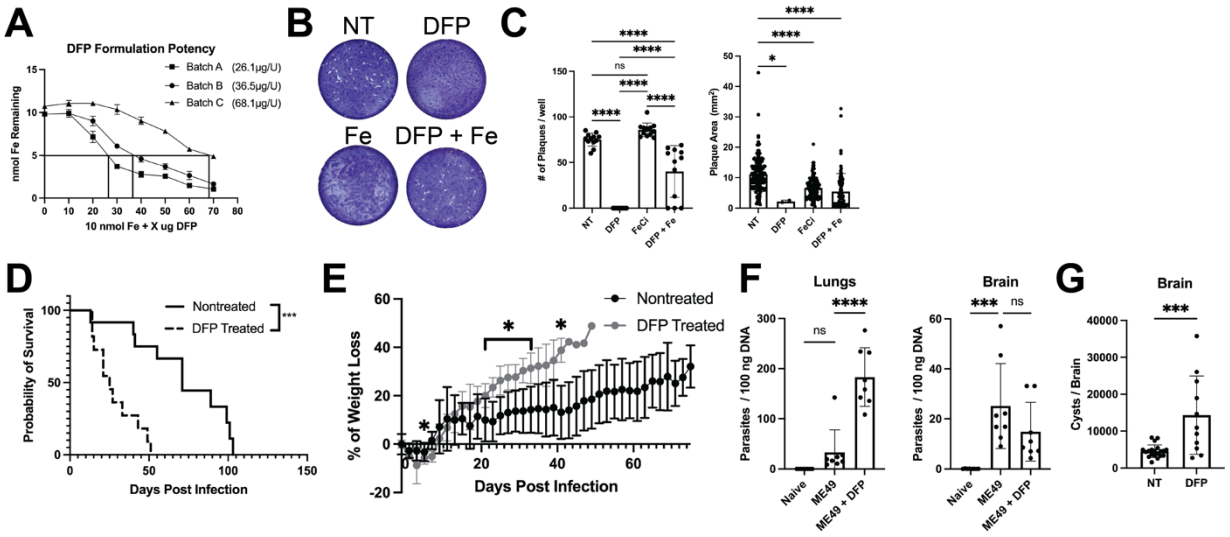

Figure 1. Iron restriction reduces *T. gondii* replication *in vitro* yet increases morbidity and mortality *in vivo*.

A) Separate lots of DFP formulations were tested for Iron-Binding Units as described. Line graph shows titration curves of DFP used to determine 50% quenching of iron. **B)** Representative plaque assays are presented of RH strain *T. gondii* infection of fibroblasts that were non-treated (NT) or treated with 1.37U DFP, 30µg ferric citrate (Fe), or 1.37U DFP and 30µg ferric citrate (DFP + Fe). **C)** Bar graphs present pooled data from two independent replicates of N=6 each for total plaque number (left) and size of plaques (right, minimum 30 plaques measured per condition if possible). **D-H)** C57BL/6 mice infected with 8 cysts ME49 strain *T. gondii* i.g. and treated i.p. with 75U DFP every other day starting the day before infection were monitored or sacrificed at the timepoints indicated. **D)** Survival of infected mice after treatment with 75U DFP. Survival graph presents data pooled from three independent experiments of N=3-5 per group. **E)** Line graph presents percentage of weight loss over time of mice after treatment with 75U DFP. Data pooled from two independent repeats of N=4-5 per group. **F)** Parasite burden at 14DPI or time of death in infected organs after treatment with 75U DFP. Bar graphs

present data from lung and brain pooled from two independent experiments of N=4 each. **G)** Brain cysts enumerated from infected mice treated with 75U DFP i.p. every other day starting on day -1 and surviving until day 35. Bar graph presents data pooled from four independent experiments but due to death of mice prior to day 35 the total sample size was 20 for NT and 11 for DFP treated groups. Bar graphs depict mean $\pm$ SD. Significance is denoted with * where $p \leq 0.05$, ** where $p \leq 0.01$, *** where $p \leq 0.005$, **** where $p \leq 0.001$, and NS where $p > 0.05$.

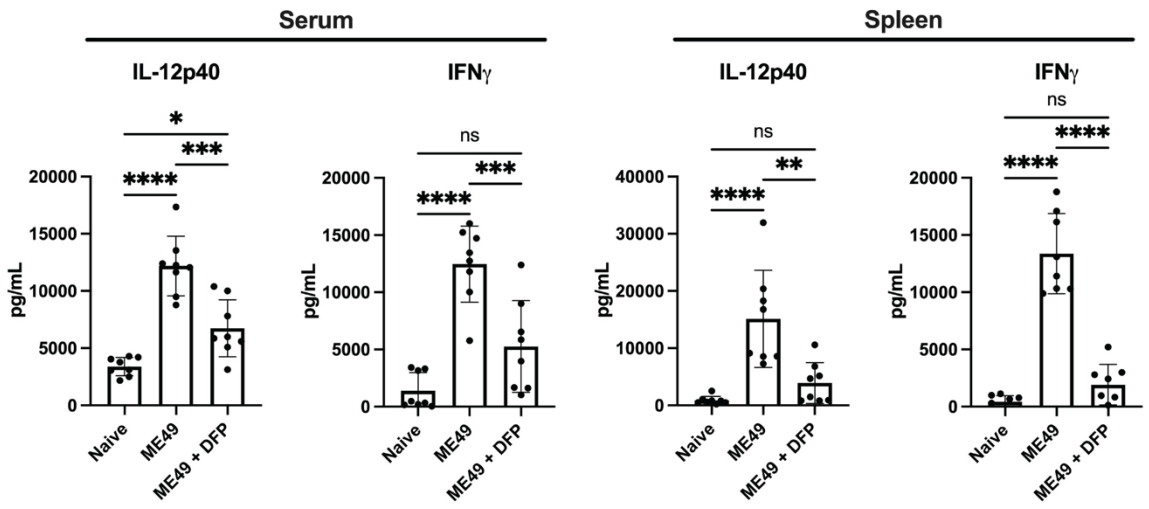

1090

1091 **Figure 2. Iron restriction lowers IL-12 and IFNγ at 5DPI of *T. gondii* infection.**

1092 Spleen cells and serum from C57BL/6 mice infected with 8 cysts ME49 I.G. and treated
1093 with 75U DFP were harvested at 5DPI. Bar graphs present results of ELISA
1094 measurements of serum levels and splenocyte production of IL-12p40 and IFNγ pooled
1095 from two independent experiments of N=4 each. All graphs depict mean ± SD.
1096 Significance is denoted with * where $p \leq 0.05$, ** where $p \leq 0.01$, *** where $p \leq 0.005$,
1097 **** where $p \leq 0.001$, and NS where $p > 0.05$.

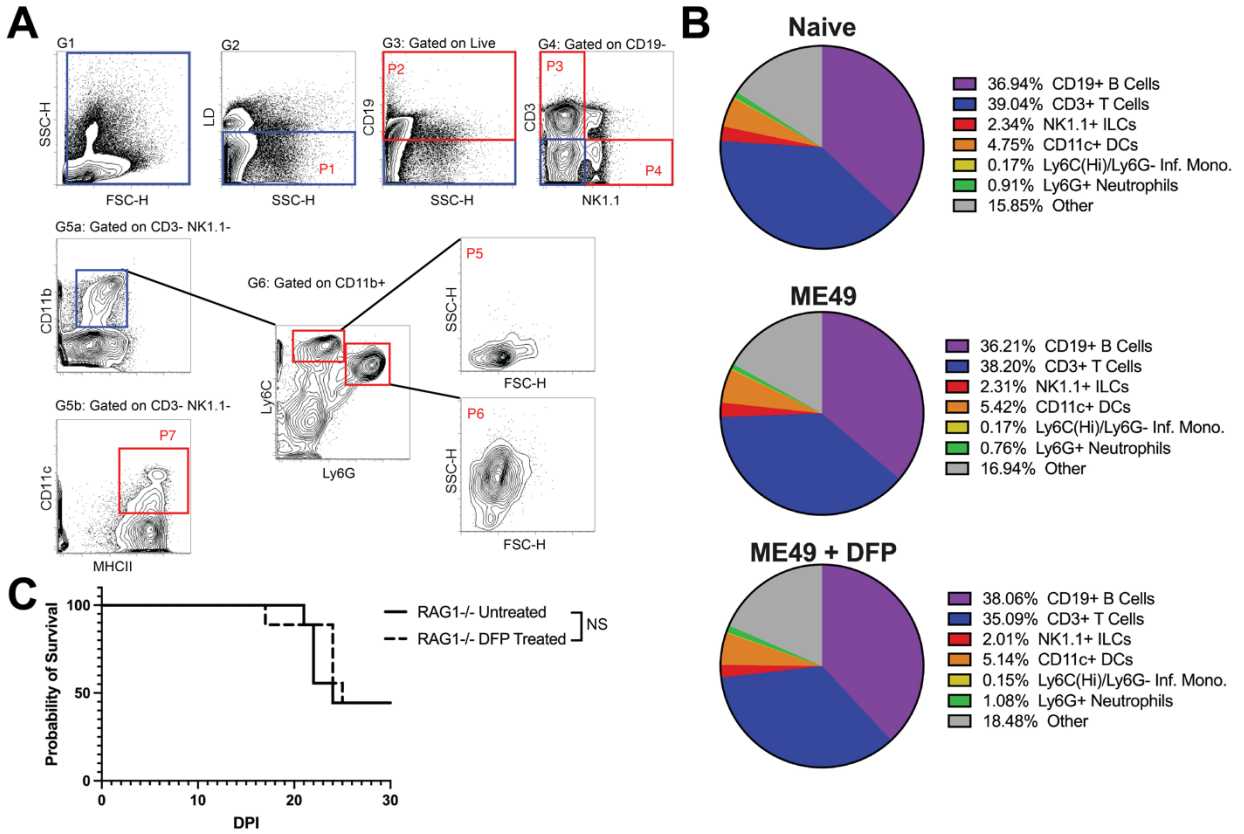

Figure 3. Iron restriction does not impact spleen cell proportions during early acute *T. gondii* infection.

C57BL/6 mice were infected orally with 8 cysts ME49 and treated with 75U DFP i.p. on days -1, 1, and 3. Splenocytes were isolated on day 5 for flow cytometric analysis. **A)** Gating strategy presents Boolean gates (denoted G and in blue boxes) and population gates (denoted P and in red boxes). Lineage negative populations were gated as Live/Dead-, CD19-, CD3-, and NK1.1-. Population gates included P1 (Total Live Cells), P2 (Live, CD19+), P3 (Live, CD19+, CD3+, NK1.1-), P4 (Live, CD19-, CD3-, NK1.1+), P5 (Lineage-, CD11b+, Ly6CHi, Ly6G-, confirmed by side scatter profile), P6 (Lineage-, CD11b+ Ly6Cint, Ly6G+, confirmed by side scatter profile), P7 (Lineage-, CD11c+, I-A/I-E+). **B)** Pie charts depict the frequency means of indicated cell populations derived from raw data (Supplemental Figure 2) pooled from three independent experiments of N=4 per

1111 group. **C)** Survival of RAG1-/- mice infected orally with 8 cysts ME49 and treated with
1112 75U DFP i.p. every other day starting the day before infection. Survival data is pooled
1113 from two independent experiments where NS indicates $p > 0.05$ by Kaplan-Meier
1114 analysis.

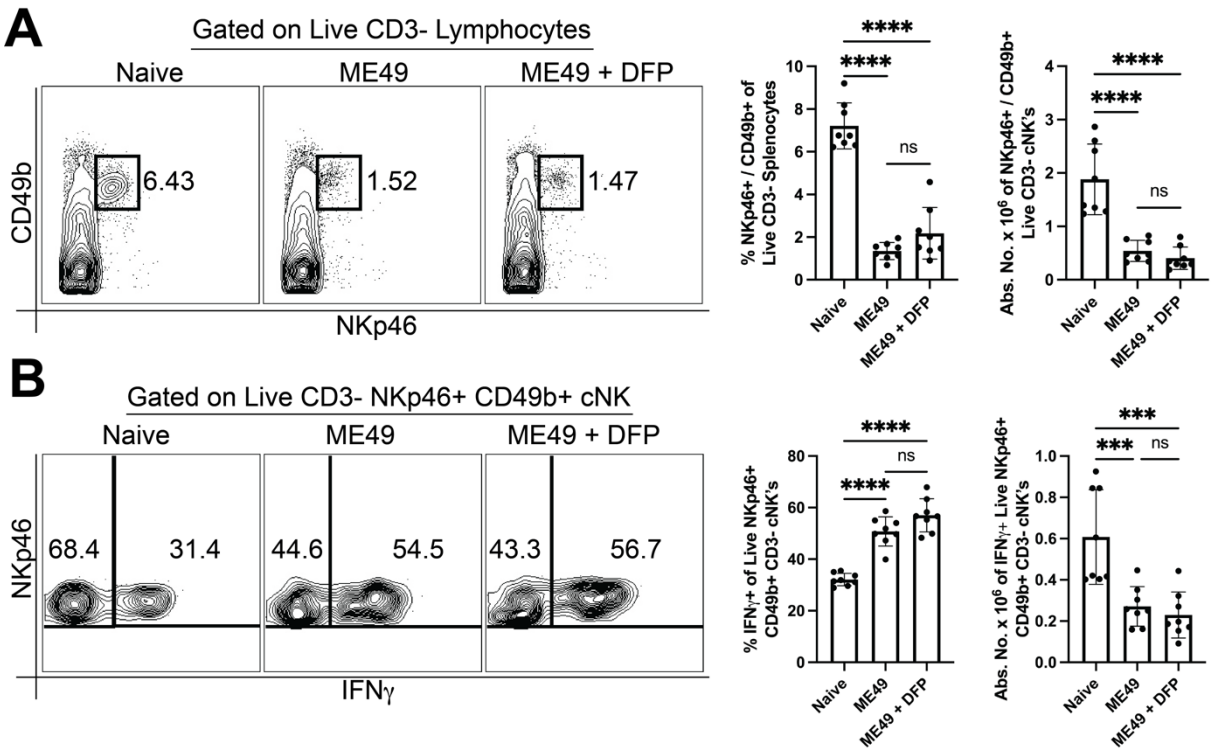

Figure 4. NK cell number and function are not affected by iron restriction during *T. gondii* infection.

C57BL/6 mice were orally infected with 8 cysts ME49 and treated with 75U DFP i.p. on days -1, 1, 3. Splenocytes were stimulated with α-NK1.1 according to the MIANKA. **A)** Bar graphs and contour plots present frequency and absolute numbers of splenic cNK cells (Live, CD3-, CD49b+, NKp46+). **B)** Bar graphs and contour plots present frequency and absolute numbers of IFNγ-producing cNK cells (Live, CD3-, CD49b+, NKp46+, IFNγ+). Data pooled from two independent experiments of N=4 per group. All graphs depict mean $\pm$ SD. Significance is denoted with * where $p \leq 0.05$, ** where $p \leq 0.01$, *** where $p \leq 0.005$, **** where $p \leq 0.001$, and NS where $p > 0.05$.

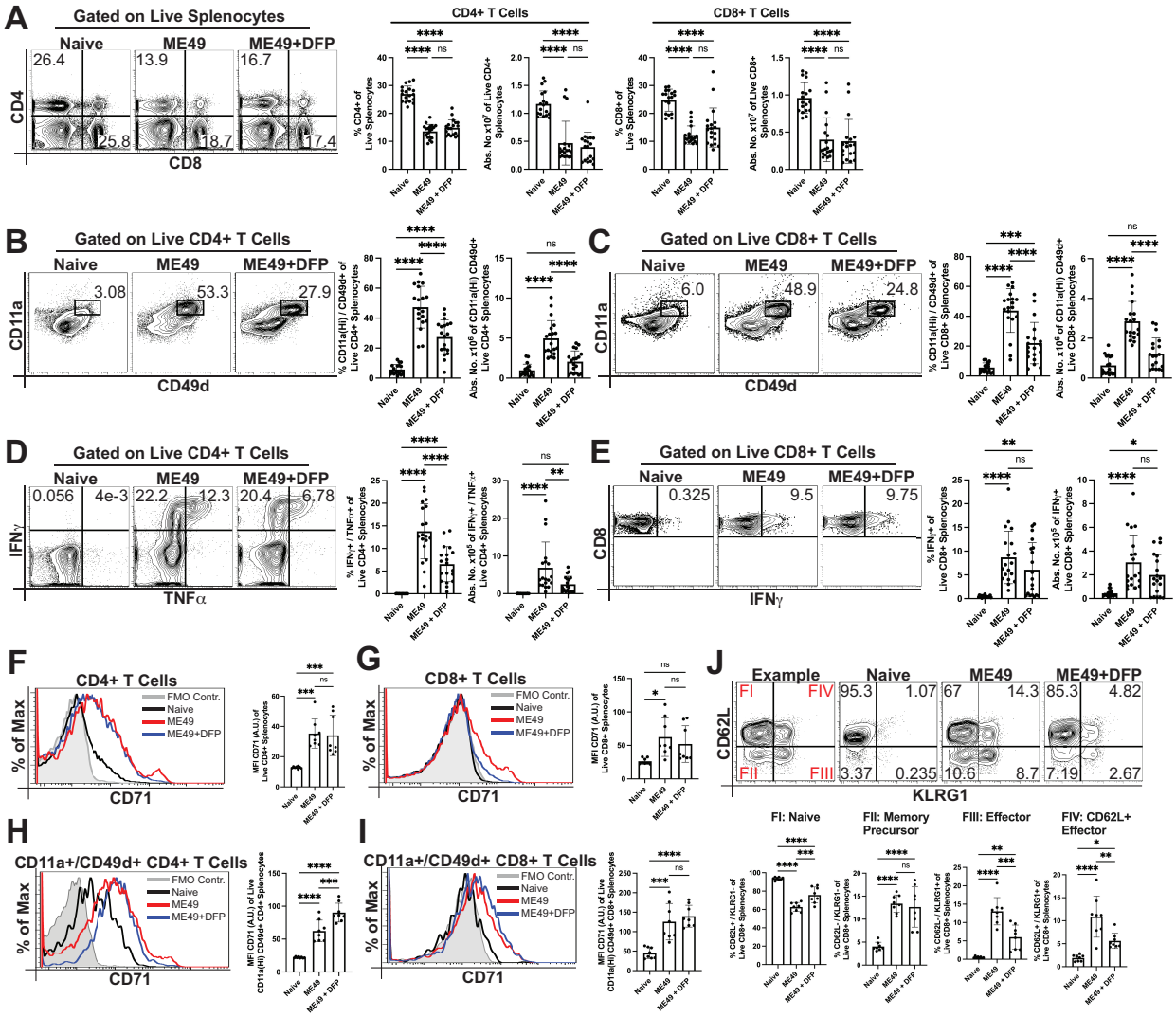

Figure 5. Iron is required for CD4+ and CD8+ T cell activation, expansion, function, and effector cell differentiation during Type II strain ME49 infection.

C57BL/6 mice were orally infected with 8 cysts ME49 strain *T. gondii* and treated with 75U DFP i.p. every other day starting the day before infection. Splenocytes were prepared for stimulation with TLA or for direct *ex vivo* flow cytometry.. **A)** Direct *ex vivo* staining of CD4 and CD8 is represented by contour plots and bar graphs presenting frequency and absolute numbers of CD4+ T cells (Live/CD4+/CD8-) or CD8+ T Cells (Live/CD4-/CD8+). **B)** Direct *ex vivo* staining of CD11a and CD49d is represented by contour plots and bar

1135 graphs presenting frequency and absolute numbers of antigen experienced CD4+ T cells
1136 (Live/CD4+/CD8-/CD11aHi/CD49d+). **C)** Direct *ex vivo* staining of CD11a and CD49d is
1137 represented by contour plots and bar graphs presenting frequency and absolute numbers
1138 of antigen experienced CD8+ T cells (Live/CD4-/CD8+/CD11aHi/CD49d+). **D)** TLA-
1139 stimulated staining of IFNγ and TNFα is represented by contour plots and bar graphs of
1140 frequency and absolute numbers of polyfunctional CD4+ T Cells (Live/CD4+/CD8-
1141 /IFNγ+/TNFα+). **E)** TLA-stimulated staining of IFNγ is represented by contour plots and
1142 bar graphs of frequency and absolute numbers of functional CD8+ T Cells (Live/CD4-
1143 /CD8+/IFNγ+). **F-I)** Direct *ex vivo* staining of CD71 is represented by histograms and bar
1144 graphs presenting the geometric mean of CD71 intensity of F) Total CD4+ T cells
1145 (Live/CD4+/CD8-), G) Total CD8+ T cells (Live/CD4-/CD8+), H) Antigen experienced
1146 CD4+ T cells (Live/CD4+/CD8-/CD11aHi/CD49d+), and I) Antigen experienced CD8+ T
1147 cells (Live/CD4-/CD8+/CD11aHi/CD49d+). **J)** Direct *ex vivo* staining of KLRG1 and
1148 CD62L on CD8+ T cells is represented by contour plots and bar graphs presenting the
1149 frequency of FI: Naïve (CD62L+/KLRG1-), FII: Memory Precursor (CD62L-/KLRG1-), FIII:
1150 Short lived Effector (CD62L-/KLRG1+), and FIV: CD62L+ Effector (CD62L+/KLRG1+)
1151 subpopulations within the Live/CD4-/CD8+ population. All data pooled from 2-5
1152 independent experiments of N=3-5 per group. All graphs depict mean ± SD. Significance
1153 is denoted with * where $p \leq 0.05$, ** where $p \leq 0.01$, *** where $p \leq 0.005$, **** where $p \leq$
1154 0.001, and NS where $p > 0.05$.

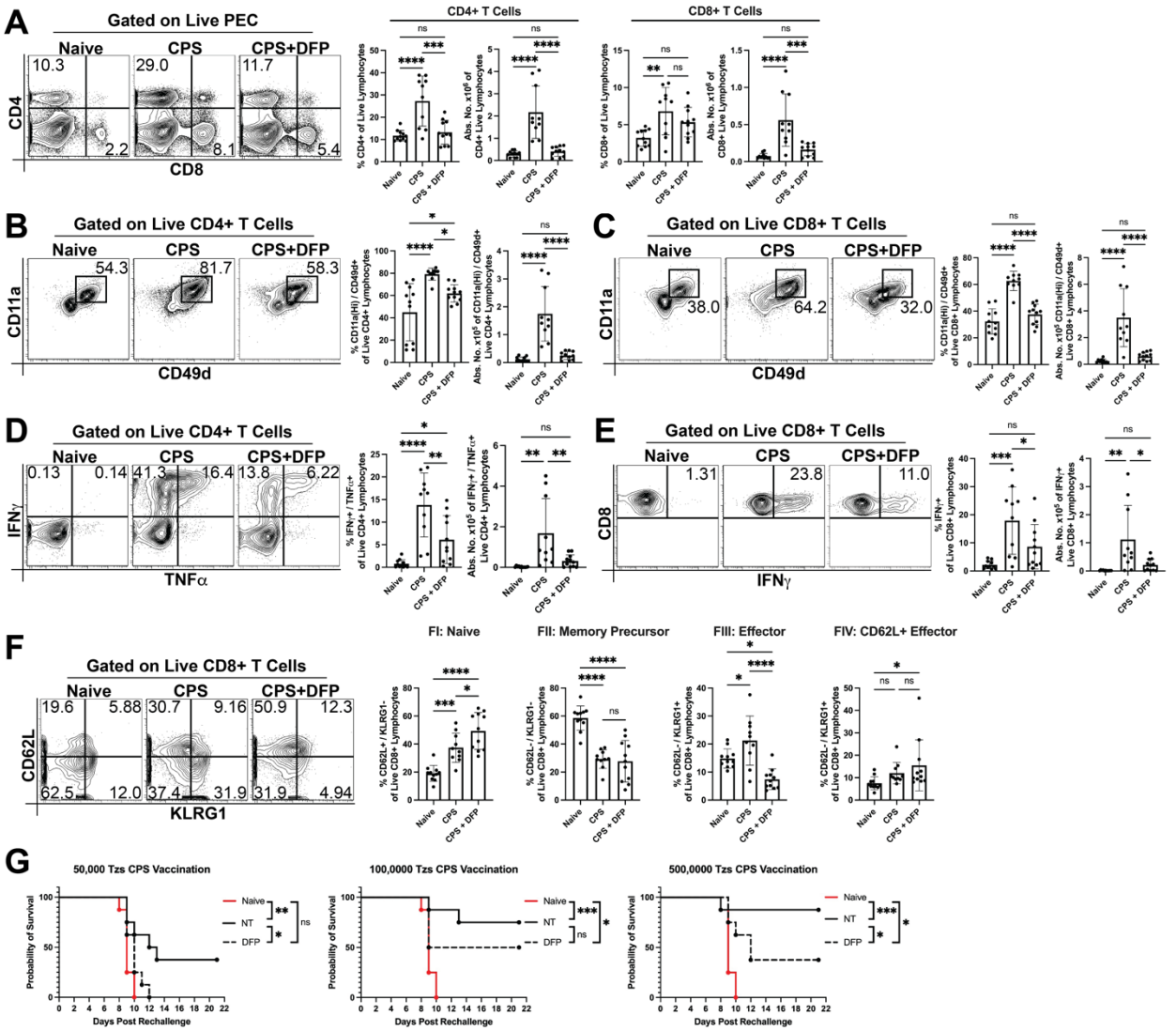

Figure 6. Inhibition of CD4+ and CD8+ T cell activation, expansion, function, and effector cell differentiation by iron restriction during vaccination is independent of antigen load.

A-F) C57BL/6 mice were infected with 1 X 10^6 tachyzoites CPS i.p. and treated with 75U DFP as described. At 7DPI, peritoneal Exudate Cells (PEC) were prepared for simulation or direct *ex vivo* staining. **A)** Direct *ex vivo* staining of CD4 and CD8 is represented by contour plots and bar graphs presenting frequency and absolute numbers of CD4+ T cells (Live/CD4+/CD8-) or CD8+ T Cells (Live/CD4-/CD8+). **B)** Direct *ex vivo* staining of CD11a

1164 and CD49d is represented by contour plots and bar graphs presenting frequency and
1165 absolute numbers of antigen experienced CD4+ T cells (Live/CD4+/CD8-
1166 /CD11aHi/CD49d+). **C)** Direct ex vivo staining of CD11a and CD49d is represented by
1167 contour plots and bar graphs presenting frequency and absolute numbers of antigen
1168 experienced CD8+ T cells (Live/CD4-/CD8+/CD11aHi/CD49d). **D)** TLA-stimulated
1169 staining of IFNγ and TNFα is represented by contour plots and bar graphs presenting
1170 frequency and absolute numbers of polyfunctional CD4+ T Cells (Live/CD4+/CD8-
1171 /IFNγ+/TNFα+). **E)** TLA-stimulated staining of IFNγ is represented by contour plots and
1172 graphs presenting frequency and absolute numbers of functional CD8+ T Cells
1173 (Live/CD4-/CD8+/IFNγ+). **F)** Direct *ex vivo* staining of KLRG1 and CD62L on CD8+ T cells
1174 is represented by contour plots and graphs presenting the frequency of FI: Naïve
1175 (CD62L+/KLRG1-), FII: Memory Precursor (CD62L-/KLRG1-), FIII: Short lived Effector
1176 (CD62L-/KLRG1+), and FIV: CD62L+ Effector (CD62L+/KLRG1+) subpopulations within
1177 the Live/CD4-/CD8+ population. **G)** C57BL/6 mice were injected with 1 X 10^4 (left), 5 X
1178 10^4 (middle), or 1 X 10^5 (right) tachyzoites of CPS strain *T. gondii* while being treated or
1179 not with 75U DFP for the first three weeks of vaccination. DFP treatment was then
1180 stopped for the last 2 weeks of vaccination allowing iron levels to recover. Graphs present
1181 survival of mice lethally challenged with 1 X 10^3 RH strain *T. gondii* two weeks after
1182 cessation of DFP treatment. All flow cytometry data are pooled from three independent
1183 experiments of N=3-4 per group. All bar graphs depict mean ± SD. Vaccination studies
1184 were conducted twice. Significance is denoted with * where $p \leq 0.05$, ** where $p \leq 0.01$,
1185 *** where $p \leq 0.005$, **** where $p \leq 0.001$, and NS where $p > 0.05$.

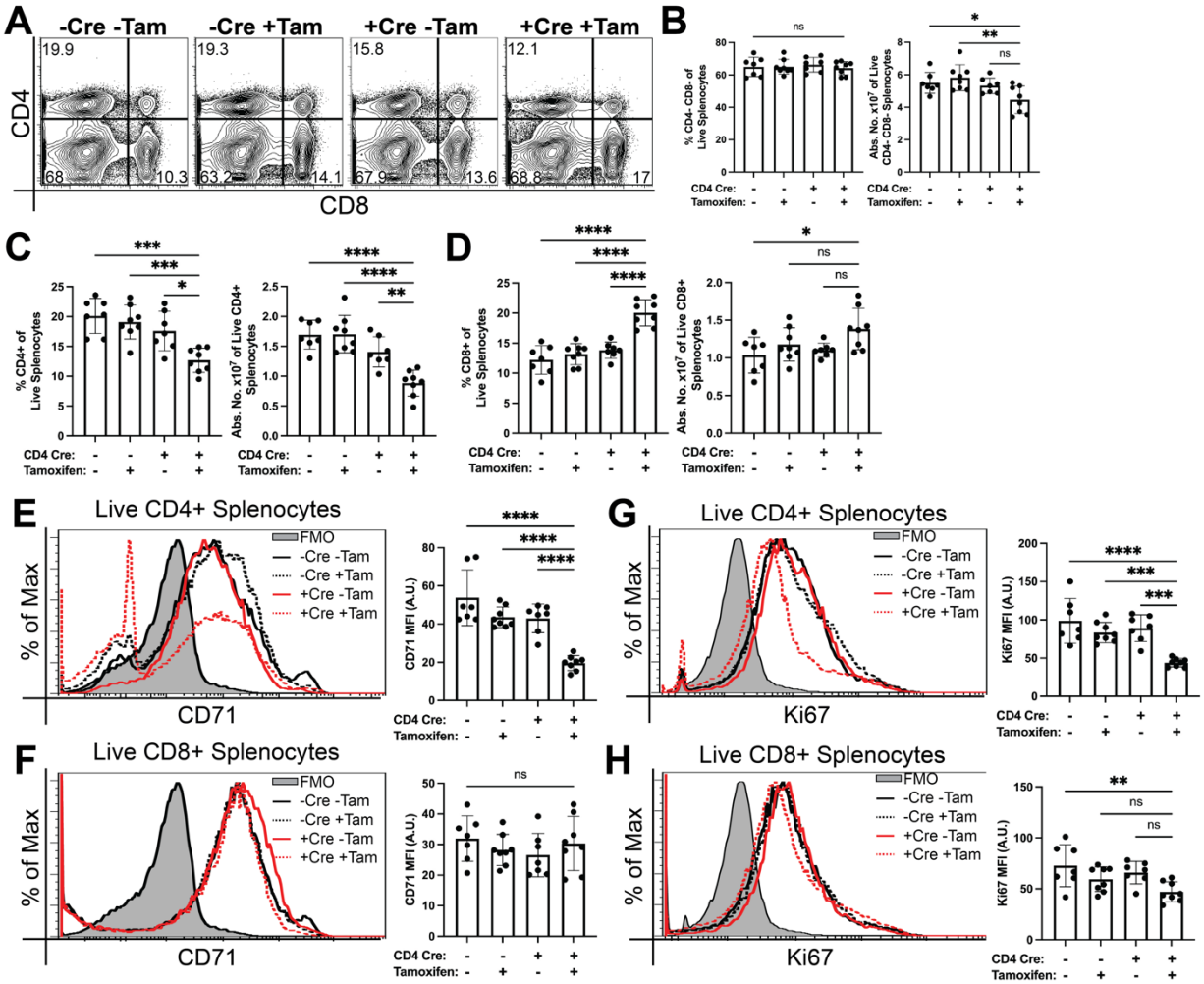

Figure 7. CD71 is required for activation and expansion of CD4+ T cells in a cell intrinsic manner during *T. gondii* infection.

CD4cCD71KO mice and littermate controls were genotyped for possession (Cre+) or not (Cre-) of CreER^{T2} recombinase under the CD4 promotor, and all possessed flanking lox sites of the endogenous CD71 gene. Cre+ and Cre- littermates were alternatively treated (Tam+) or not (Tam-) with 100mg/kg tamoxifen i.p. daily for five days prior to oral infection with 8 cysts ME49. Splenocytes were harvested 10DPI for direct *ex vivo* staining according to the MIATA. **A-D)** Direct *ex vivo* staining of CD4 and CD8 is represented by contour plots and bar graphs presenting frequency and absolute numbers of B) non-T

1196 Cells (Live/CD4-/CD8-), C) CD4+ T cells (Live/CD4+/CD8-), and D) CD8+ T cells
1197 (Live/CD4-/CD8+). **E-F)** Direct *ex vivo* staining of CD71 is represented by histograms and
1198 bar graphs presenting geometric mean of CD71 intensity in E) CD4+ T Cells
1199 (Live/CD4+/CD8-) and F) CD8+ T cells (Live/CD4-/CD8+). **G-H)** Direct *ex vivo* staining of
1200 Ki67 is represented by histograms and bar graphs presenting geometric mean of Ki67
1201 intensity in G) CD4+ T Cells (Live/CD4+/CD8-) and H) CD8+ T cells (Live/CD4-/CD8+).
1202 All data pooled from two independent experiments of N=3-4 per group. Bar graphs depict
1203 mean $\pm$ SD. Significance is denoted with * where $p \leq 0.05$, ** where $p \leq 0.01$, *** where
1204 $p \leq 0.005$, **** where $p \leq 0.001$, and NS where $p > 0.05$.

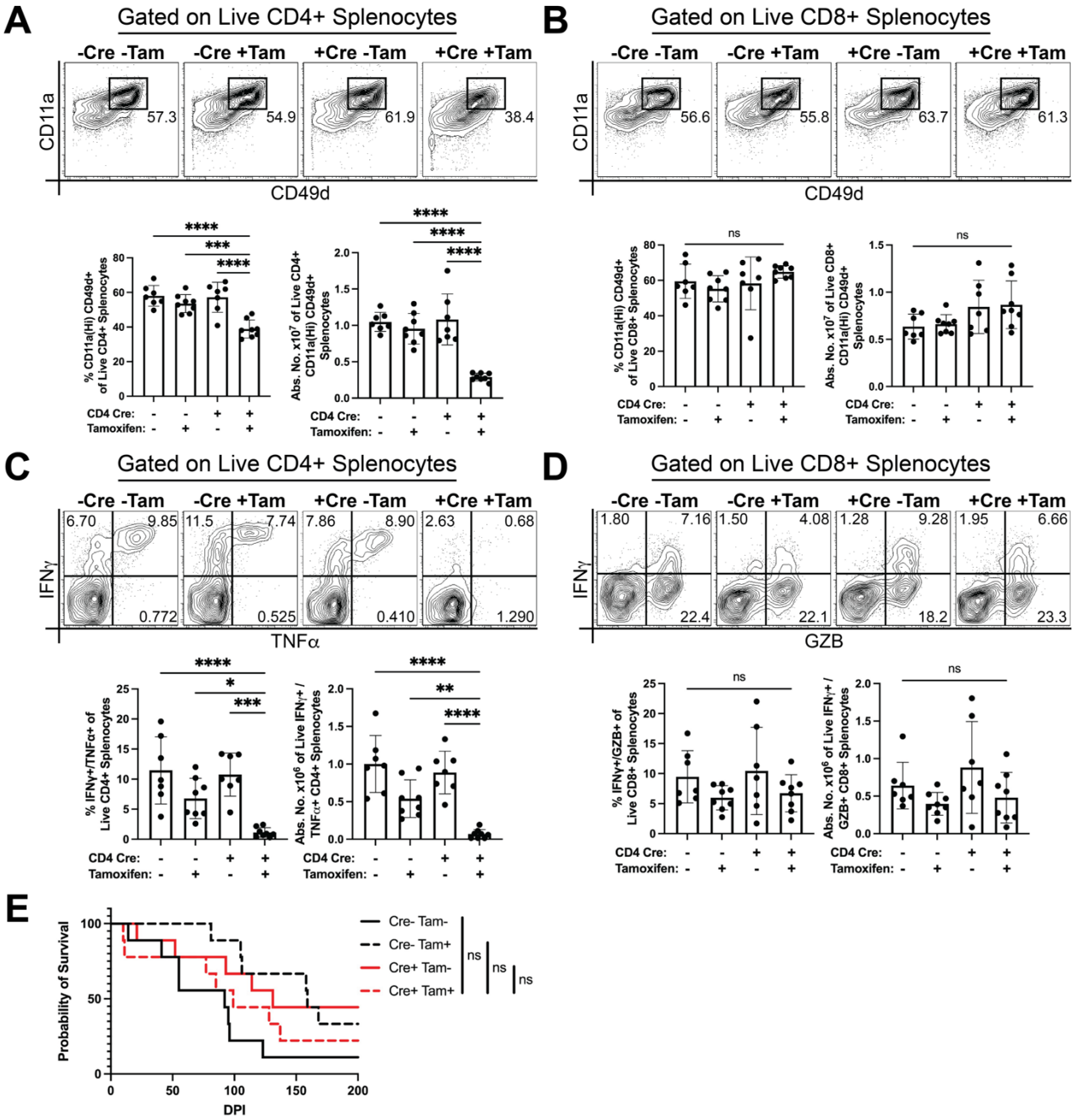

Figure 8. CD71 is required to increase antigen experience and polyfunctional responses of CD4+ T cells in *T. gondii* infection

CD4cCD71KO mice and littermate controls were genotyped for possession (Cre+) or not (Cre-) of CreER^{T2} recombinase under the CD4 promotor, and all possessed flanking lox

1210 sites of the endogenous CD71 gene. Cre+ and Cre- littermates were alternatively treated
1211 (Tam+) or not (Tam-) with 100mg/kg tamoxifen i.p. daily for five days prior to oral infection
1212 with 8 cysts ME49. Splenocytes were harvested 10DPI for stimulation or direct *ex vivo*
1213 staining according to the MIATA. **A)** Direct *ex vivo* staining of CD11a and CD49d is
1214 represented by contour plots and bar graphs presenting frequency and absolute numbers
1215 of antigen experienced CD4+ T cells (Live/CD4+/CD8-/CD11aHi/CD49d+). **B)** Direct *ex*
1216 *vivo* staining of CD11a and CD49d is represented by contour plots and bar graphs
1217 presenting frequency and absolute numbers of antigen experienced CD8+ T cells
1218 (Live/CD4-/CD8+/CD11aHi/CD49d). **C)** TLA-stimulated staining of IFNγ and TNFα is
1219 represented by contour plots and bar graphs presenting frequency and absolute numbers
1220 of polyfunctional CD4+ T Cells (Live/CD4+/CD8-/IFNγ+/TNFα+). **D)** TLA-stimulated
1221 staining of IFNγ is represented by contour plots and bar graphs presenting frequency and
1222 absolute numbers of polyfunctional CD8+ T Cells (Live/CD4-/CD8+/IFNγ+/GZB+). **E)**
1223 Survival of ME49 infected CD4cCD71KO mice and littermate controls treated with
1224 tamoxifen. Survival data pooled from two independent experiments of N=4-5 per group
1225 and analyzed by Kaplan-Meier statistics where NS indicates $p > 0.05$. All bar graphs
1226 pooled from two independent experiments of N=3-4 per group and depict mean $\pm$ SD.
1227 Bar graph significance is indicated with * where $p \leq 0.05$, ** where $p \leq 0.01$, *** where p
1228 ≤ 0.005, **** where $p \leq 0.001$, and NS where $p > 0.05$.

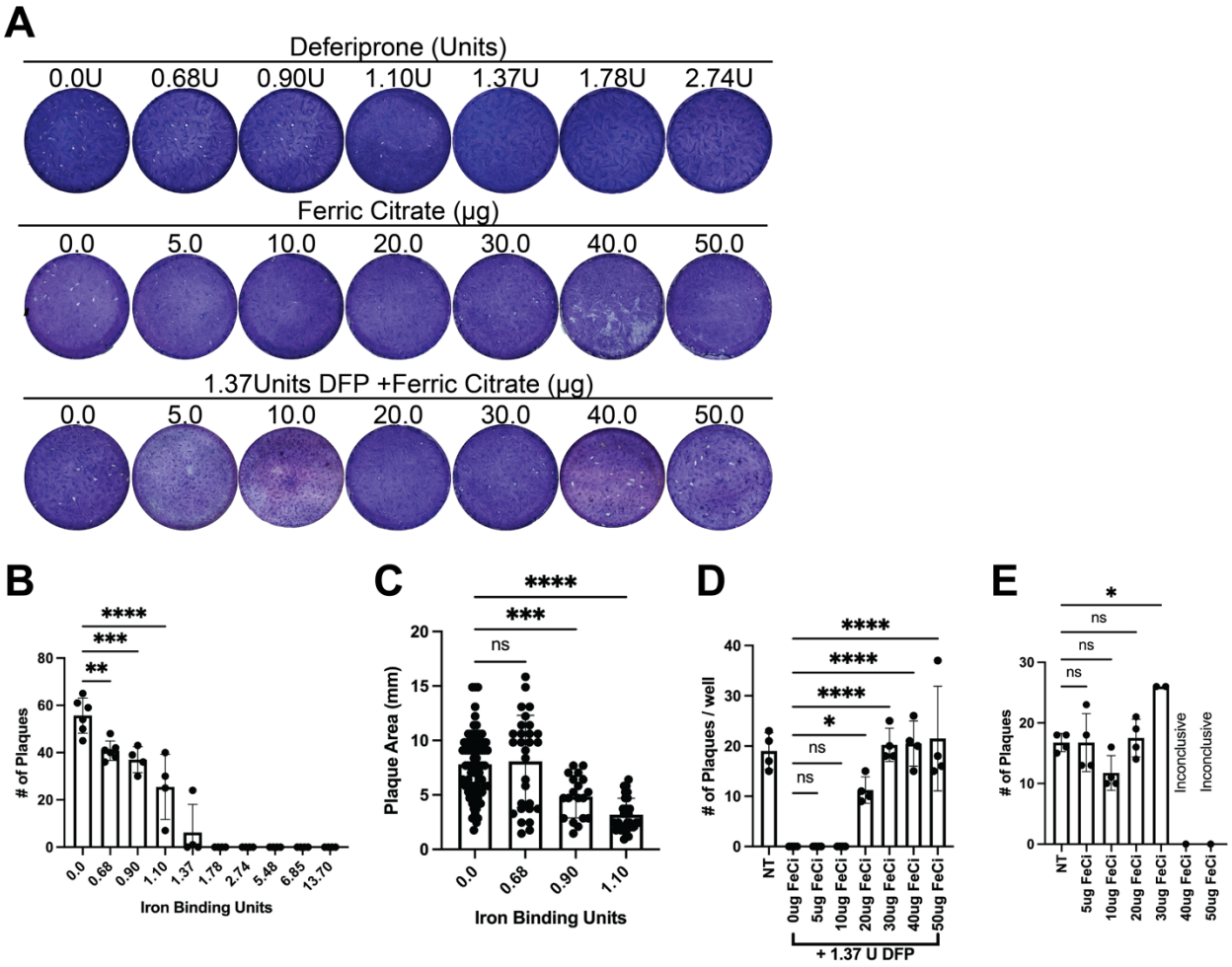

Supplemental Figure 1. Titration of deferiprone and ferric citrate in plaque assays. The growth rate of RH strain *T. gondii* treated with indicated amounts of DFP or ferric citrate was determined by plaque assay. **A)** Shown are representative plaques formed by RH at indicated levels of DFP *(top),* ferric citrate *(middle)*, and ferric citrate + 1.37U DFP *(bottom).* **B)** Bar graph presents the number of RH plaques formed when treated with indicated doses of DFP. **C)** Bar graph presents the size of RH plaques formed when treated with indicated doses of DFP. **D)** Bar graph shows the number of plaques formed after supplementation of 1.37U DFP with indicated amounts of ferric citrate. **E)** Bar graph presents the number of plaques formed when supplemented with indicated amounts of ferric citrate alone. Data representative of two independent experiments. Bar graphs show

1240 mean $\pm$ SD. Significance is denoted with * where $p \leq 0.05$, ** where $p \leq 0.01$, *** where

1241 $p \leq 0.005$, **** where $p \leq 0.001$, and NS where $p > 0.05$.

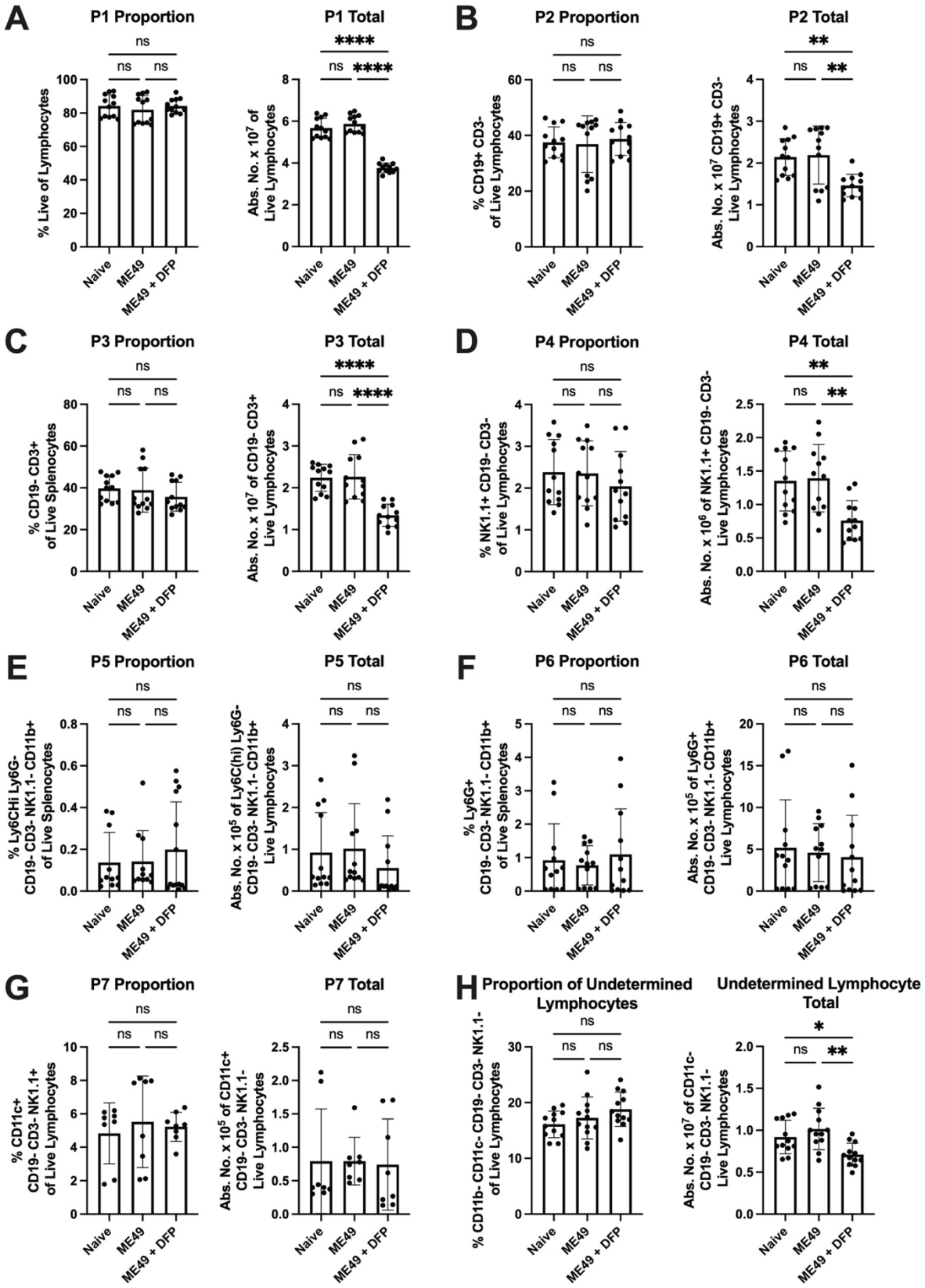
A
P1 Proportion
% Live of Lymphocytes
P1 Total
Abs. No. x 10^7 of Live Lymphocytes
B
P2 Proportion
% CD19+ CD3- of Live Lymphocytes
P2 Total
Abs. No. x 10^7 CD19+ CD3- Live Lymphocytes
C
P3 Proportion
% CD19- CD3+ of Live Splenocytes
P3 Total
Abs. No. x 10^7 of CD19- CD3+ Live Lymphocytes
D
P4 Proportion
% NK1.1+ CD19- CD3- of Live Lymphocytes
P4 Total
Abs. No. x 10^6 of NK1.1+ CD19- CD3- Live Lymphocytes
E
P5 Proportion
% Ly6CHi Ly6G- CD19- CD3- NK1.1- CD11b+ of Live Splenocytes
P5 Total
Abs. No. x 10^5 of Ly6C(hi) Ly6G- CD19- CD3- NK1.1- CD11b+ Live Lymphocytes
F
P6 Proportion
% Ly6G+ CD19- CD3- NK1.1- CD11b+ of Live Splenocytes
P6 Total
Abs. No. x 10^5 of Ly6G+ CD19- CD3- NK1.1- CD11b+ Live Lymphocytes
G
P7 Proportion
% CD11c+ CD19- CD3- NK1.1+ of Live Lymphocytes
P7 Total
Abs. No. x 10^5 of CD11c+ CD19- CD3- NK1.1- Live Lymphocytes
H
Proportion of Undetermined Lymphocytes
% CD11b- CD11c- CD19- CD3- NK1.1- of Live Lymphocytes
Undetermined Lymphocyte Total
Abs. No. x 10^7 of CD11c- CD19- CD3- NK1.1- Live Lymphocytes
ns
****
**
*
Naive
ME49
ME49 + DFP

1242

1243 **Supplemental Figure 2. Iron restriction does not impact splenic proportions at 5DPI**
1244 **of *T. gondii* infection.**

1245 C57BL/6 mice were infected orally with 8 cysts ME49 and treated with 75U DFP i.p. on
1246 days -1, 1, and 3. Splenocytes were isolated on day 5 for flow cytometric analysis. Bar
1247 graphs present frequency and absolute numbers of the following populations gated
1248 according to Figure 3A: **A)** P1 (Live Cells), **B)** P2 (Live, CD19+), **C)** P3 (Live, CD19+,
1249 CD3+, NK1.1-), **D)** P4 (Live, CD19-, CD3-, NK1.1+), **E)** P5 (Lineage-, CD11b+, Ly6CHi,
1250 Ly6G-, confirmed by side scatter profile), **F)** P6 (Lineage-, CD11b+ Ly6Cint, Ly6G+,
1251 confirmed by side scatter profile), **G)** P7 (Lineage-, CD11c+, I-A/I-E+), and **H)** P8
1252 (Lineage- CD11b- CD11c-). Data pooled from three independent experiments. Bar graphs
1253 depict mean $\pm$ SD. Significance is denoted with * where $p \leq 0.05$, ** where $p \leq 0.01$, ***
1254 where $p \leq 0.005$, **** where $p \leq 0.001$, and NS where $p > 0.05$.

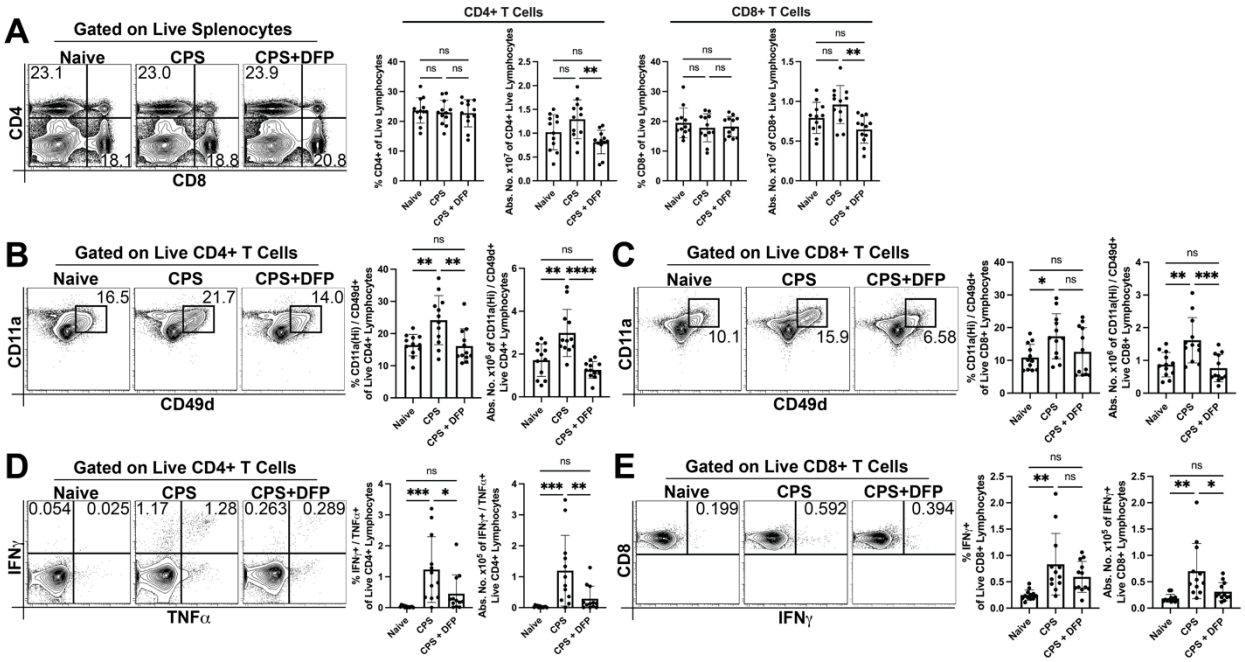

Supplemental Figure 3. Inhibition of splenic T cell antigen experience and functionality by iron restriction during vaccination is independent of antigen load. C57BL/6 mice infected with 1 X 10^6 tachyzoites CPS i.p. and treated with 75U DFP as described in the Materials and Methods. Animals were sacrificed and splenocytes were prepared for stimulation and for direct *ex vivo* staining. **A)** Direct *ex vivo* staining of CD4 and CD8 is represented by contour plots and bar graphs presenting frequency and absolute numbers of CD4+ T cells (Live/CD4+/CD8-) or CD8+ T Cells (Live/CD4-/CD8+). **B)** Direct *ex vivo* staining of CD11a and CD49d is represented by contour plots and bar graphs presenting frequency and absolute numbers of antigen experienced CD4+ T cells (Live/CD4+/CD8-/CD11aHi/CD49d+). **C)** Direct *ex vivo* staining of CD11a and CD49d is represented by contour plots and bar graphs presenting frequency and absolute numbers of antigen experienced CD8+ T cells (Live/CD4-/CD8+/CD11aHi/CD49d+). **D)** TLA-stimulated staining of IFNγ and TNFα is represented by contour plots and bar graphs of frequency and absolute numbers of polyfunctional CD4+ T Cells (Live/CD4+/CD8-

1270 /IFNγ+/TNFα+). **E)** TLA-stimulated staining of IFNγ is represented by contour plots and
1271 bar graphs of frequency and absolute numbers of functional CD8+ T Cells (Live/CD4-
1272 /CD8+/IFNγ+). All data pooled from three independent experiments of N=4 per group. Bar
1273 graphs depict mean $\pm$ SD. Significance is denoted with * where $p \leq 0.05$, ** where $p \leq$
1274 0.01, *** where $p \leq 0.005$, **** where $p \leq 0.001$, and NS where $p > 0.05$.

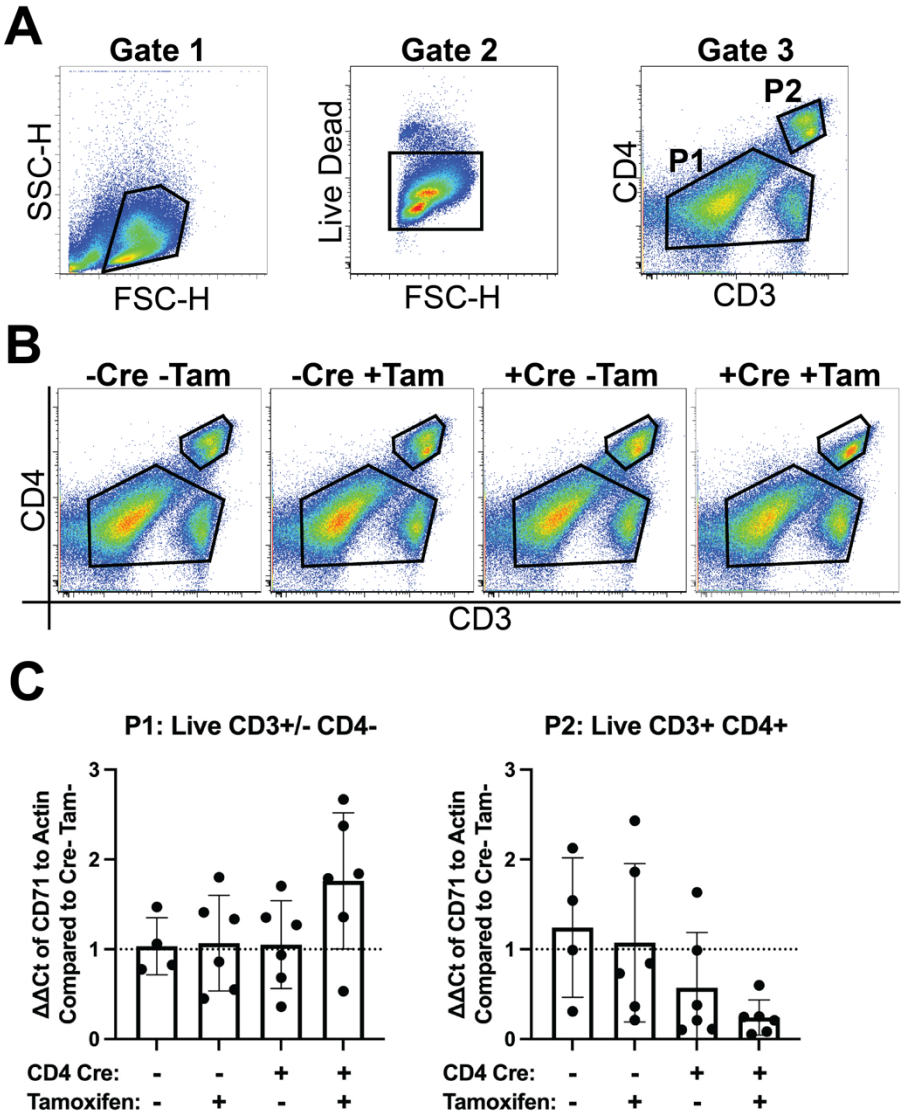

Supplemental Figure 4. Conditional knockout of iron uptake receptor CD71 in CD4+ T cells

CD4cCD71KO mice and littermate controls were genotyped for possession (Cre+) or not (Cre-) of CreER^{T2} recombinase under the CD4 promotor, and all possessed flanking lox sites of the endogenous CD71 gene. Cre+ and Cre- littermates were alternatively treated (Tam+) or not (Tam-) with 100mg/kg tamoxifen i.p. daily for five days prior to oral infection with 8 cysts ME49. Splenocytes were harvested 10DPI for FACS and RT-PCR according to the MIATA. **A)** FACS gating strategy used for sorting of non CD4+ T

1284 cells (P1: Live, CD3+/-, CD4-) and CD4+ T cells (P2: Live, CD3+, CD4+). **B)**
1285 Pseudocolored dotplots represent FACS sorting populations for each group. **C)** Bar
1286 graphs present relative mRNA expression of CD71 compared to actin and normalized to
1287 the Cre- Tam- littermate control. The left graph shows CD71 mRNA expression of P1
1288 sorted cells and the right graph shows CD71 mRNA expression of P2 sorted cells. All
1289 data was pooled from two independent experiments of N=1-4 per group and graphs are
1290 mean $\pm$ SD. No comparisons were statistically significant.